Table 3.1 Experimental, Low Speed NACA Airfoil Data for Smooth Leading Edges

(Note: Data reproduced from Reference 3.1 for $R_N = 9 \times 10^6$)

Airfoil	α_0 (deg)	$\bar{c}_{m_0}$	c_{l_α} (1/deg)	$\bar{x}_{ac}$	$\alpha_{c_{l_{max}}}$ (deg)	$c_{l_{max}}$	α^* (deg)
0006	0	0	0.108	0.250	9.0	0.92	9.0
0009	0	0	0.109	0.250	13.4	1.32	11.4
1408	–0.8	–0.023	0.109	0.250	14.0	1.35	10.0
1410	–1.0	–0.020	0.108	0.247	14.3	1.50	11.0
1412	–1.1	–0.025	0.108	0.252	15.2	1.58	12.0
2412	–2.0	–0.047	0.105	0.247	16.8	1.68	9.5
2415	–2.0	–0.049	0.106	0.246	16.4	1.63	10.0
2418	–2.3	–0.050	0.103	0.241	14.0	1.47	10.0
2421	–1.8	–0.040	0.103	0.241	16.0	1.47	8.0
2424	–1.8	–0.040	0.098	0.231	16.0	1.29	8.4
23012	–1.4	–0.014	0.107	0.247	18.0	1.79	12.0
23015	–1.0	–0.007	0.107	0.243	18.0	1.72	10.0
23018	–1.2	–0.005	0.104	0.243	16.0	1.60	11.8
23021	–1.2	0	0.103	0.238	15.0	1.50	10.3
23024	–0.8	0	0.097	0.231	15.0	1.40	9.7
64–006	0	0	0.109	0.256	9.0	0.80	7.2
64–009	0	0	0.110	0.262	11.0	1.17	10.0
64_1–012	0	0	0.111	0.262	14.5	1.45	11.0
64_1–212	–1.3	–0.027	0.113	0.262	15.0	1.55	11.0
64_1–412	–2.6	–0.065	0.112	0.267	15.0	1.67	8.0
64–206	–1.0	–0.040	0.110	0.253	12.0	1.03	8.0
64–209	–1.5	–0.040	0.107	0.261	13.0	1.40	8.9
64–210	–1.6	–0.040	0.110	0.258	14.0	1.45	10.8
64A010	0	0	0.110	0.253	12.0	1.23	10.0
64A210	–1.5	–0.040	0.105	0.251	13.0	1.44	10.0
64A410	–3.0	–0.080	0.100	0.254	15.0	1.61	10.0
64_1A212	–2.0	–0.040	0.100	0.252	14.0	1.54	11.0
64_2A215	–2.0	–0.040	0.095	0.252	15.0	1.50	12.0

Note: For definition of symbols, see the list of Symbols

3.3.3 PITCHING MOMENT CURVE: c_m VERSUS c_l or c_m VERSUS α

Figure 3.5a shows typical airfoil data for c_m versus c_l and c_m versus α .

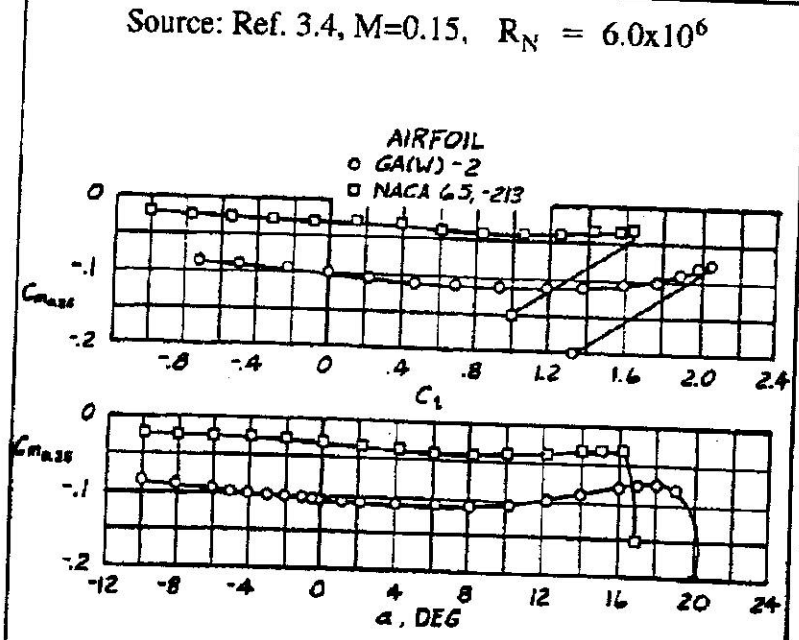

Figure 3.5a Pitching Moment Coefficient Plots for Two Airfoils

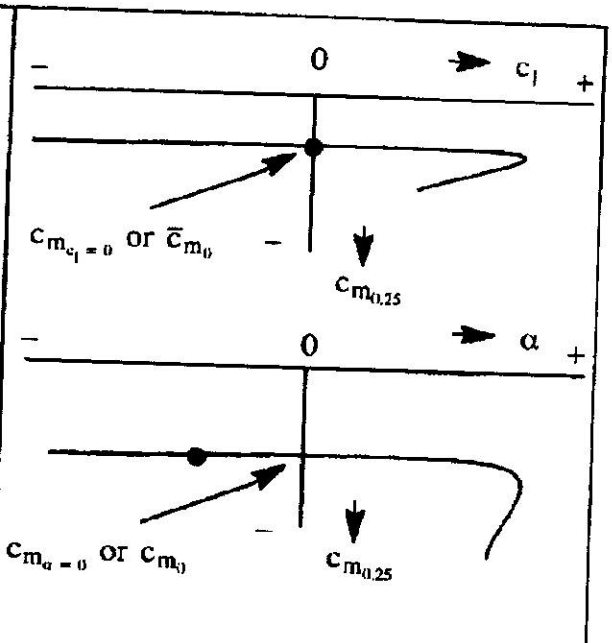

Figure 3.5b Generic Plots of Pitching Moment Coefficient Versus Lift Coefficient and Versus Angle of Attack

The magnitude of the pitching moment coefficient, c_m depends on the location of the moment reference center. This moment reference center is normally identified in a subscript to c_m .

In Figure 3.5a the moment reference center is the quarter chord point, identified in the subscript as 0.25c or simply 0.25. Generic plots of c_m versus c_l and c_m versus α are shown in Figure 3.5b. Numerical values for the parameter c_{m_0} are given in Table 3.1 for several types of airfoil.

A very important reference point on an airfoil is its so–called aerodynamic center or a.c. The aerodynamic center is defined as that point about which the variation of the pitching moment coefficient with angle of attack is zero. To find the a.c., assume that in some experimental set–up the moment reference center was selected to be a distance x from the leading edge. Figure 3.6 shows the corresponding geometry. Neglecting the moment contribution due to drag it is seen that:

$$c_{m_{ac}}\bar{q}c^2 = c_{m_x}\bar{q}c^2 + c_l\bar{q}c(x_{ac} - x) \qquad (3.19)$$

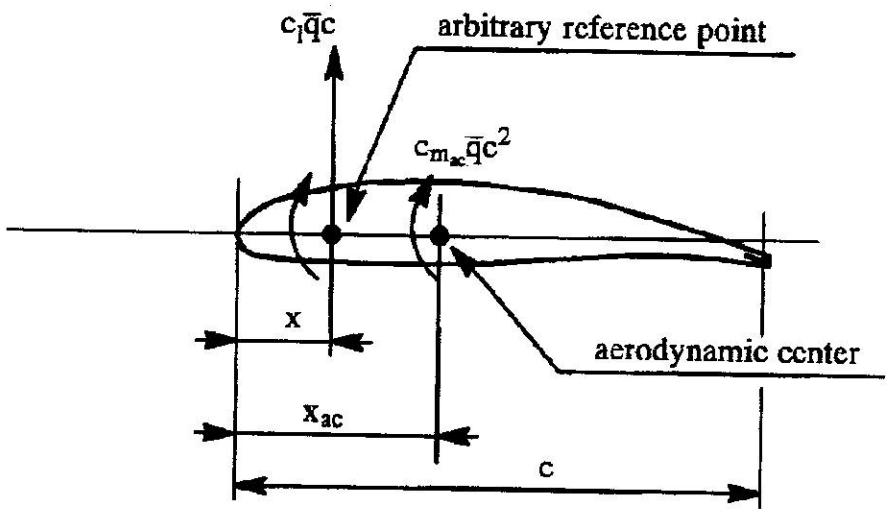

Figure 3.6 Geometry for Finding the Aerodynamic Center

$$c_{m_{ac}} = c_{m_x} + c_l\left(\frac{x_{ac} - x}{c}\right) \tag{3.20}$$

By definition, $c_{m_{ac}}$ is independent of the angle of attack, α, and therefore:

$$\frac{\partial c_{m_{ac}}}{\partial \alpha} = 0 = \frac{\partial c_{m_x}}{\partial \alpha} + \frac{\partial c_l}{\partial \alpha}\left(\frac{x_{ac} - x}{c}\right) \tag{3.21}$$

From this it follows that:

$$\frac{x_{ac}}{c} = \frac{x}{c} - \frac{\partial c_{m_x}}{\partial c_l} \tag{3.22}$$

Using experimental data of c_{m_x} versus c_l it is therefore possible to compute the location of the aerodynamic center, x_{ac} . From experimental data taken at low subsonic Mach numbers it is normally found that the aerodynamic center is at the quarter chord point: $\frac{x_{ac}}{c} \approx 0.25$.

3.4 AIRFOIL PRESSURE DISTRIBUTION

The pressure distribution over an airfoil is important for load calculations and for control surface hinge moment calculations. The pressure distribution is normally expressed in terms of the so-called pressure coefficient, c_p , which is defined as:

$$c_p = \frac{p - p_\infty}{\bar{q}_\infty} \tag{3.23}$$

$$c_{d_{min}}(\text{full scale}) = c_{d_{min}}(\text{model}) - \Delta c_{d_{min}} \tag{3.40}$$

where:

$$\Delta c_{d_{min}} = 2(\text{S.F.})[c_f(\text{model}) - c_f(\text{full scale})] \tag{3.41}$$

There still do not exist accurate theoretical methods for correcting the maximum lift coefficient from tunnel data to full scale. Jacobs and Sherman have shown some experimental results for the Reynolds number effect on $c_{l_{max}}$ for several NACA airfoils (Ref. 3.8). Additional data can be found in Ref. 3.9. Most aircraft manufacturers have their own in–house correction procedures for extrapolating tunnel $c_{l_{max}}$ data to full scale. Such procedures are then based upon their experience obtained in comparing model and airplane data.

3.7 DESIGN OF AIRFOILS

Because lifting surfaces (such as wings, tails, canards and pylons) can be thought of as spanwise arrangements of airfoils, the basic characteristics of airfoils have a major effect on the behavior of lifting surfaces. It is therefore important to be aware of those airfoil characteristics which have the potential of being 'driving' factors in airplane lift, drag, and pitching moment.

To design an airfoil for any specific requirement involving lift, drag or pitching moment, several effects of airfoil geometry on airfoil aerodynamics should be understood. It has been found that the most important geometric parameters are:

1) maximum thickness ratio, $(t/c)_{max}$
2) shape of the mean line (also referred to as camber). If the mean line is a straight line, the airfoil is said to be symmetrical.
3) leading edge shape or Δy parameter and leading edge radius (l.e.r.)
4) trailing edge angle, ϕ_{TE}

Figure 3.15 provides a geometric interpretation for these parameters, most of which were also defined in Figure 3.1. The reader should consult Ref. 3.1 for a detailed discussion of airfoil parameters and airfoil characteristics. Ref. 3.1 also contains a large body of experimental data on a variety of NACA airfoils (NACA = National Advisory Committee on Aeronautics, predecessor of NASA, the National Acronautics and Space Administration). In addition, this reference contains explanations for the numerical designations used with all NACA airfoils. Table 3.2 defines the most important NACA airfoil designations.

It is noted that the NACA 6–series airfoils were designed to have mean camber lines which produce a near uniform chordwise loading from the leading edge to a point x/c = a, and a linearly decreasing load from this point to the trailing edge. Any time this condition is met, the corresponding a–value is given after the airfoil designation.

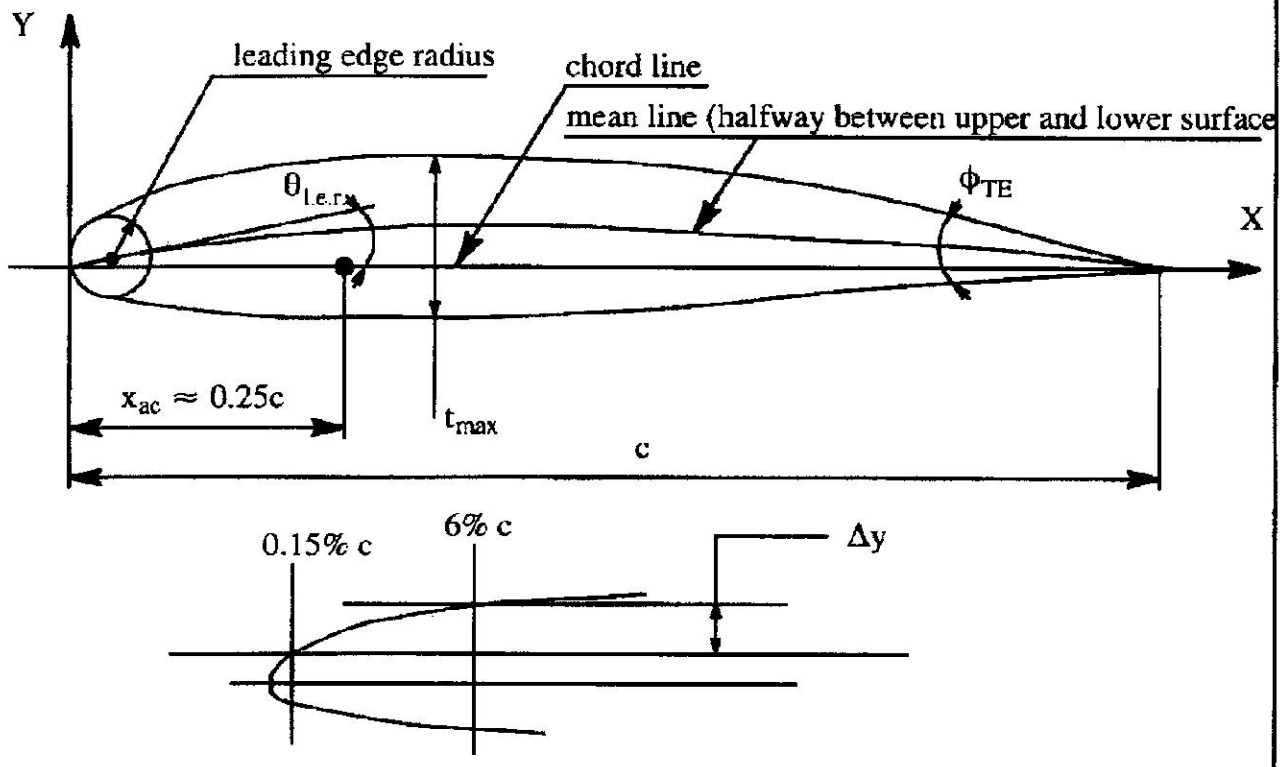

Figure 3.15 Definition of Important Airfoil Geometric Parameters

Examples are: NACA 66(215)–216 with a = 0.6 and NACA 65(318)–217 with a = 0.5. These two examples represent airfoils with thickness distributions obtained by linearly increasing or decreasing the ordinates of the originally derived distribution. In the last example, the airfoil has a 17% thickness ratio. Its ordinates were derived from the airfoil with 18% thickness distribution. The digit 3 represents in tenths, one half of the extent of the low drag range. When this digit is omitted, it implies that the low drag range is less than 0.1.

Since the late 1950's NASA has engaged in the design of airfoils for transonic transport and fighter applications. These so–called supercritical airfoils have a higher M_{dd} value than the conventional NACA 6–series airfoils as illustrated in Figure 3.13. These supercritical airfoils are characterized by very little camber in the forward portion. On the other hand, the rearward portion is severely cambered. Figure 3.16 presents an example of a supercritical airfoil.

During the course of these recent airfoil research activities, new airfoils for lower speed applications have also been derived. Examples are the low–speed airfoils, such as LS(1)–0417 and LS(1)–0413, the medium speed airfoils, such as MS(1)–0313 and natural laminar flow airfoils, such as NLF(1)–416. The LS(1)–0417 airfoil is also known as the GA(W)–1 airfoil (W stands for Whitcomb) and the LS(1)–0413 airfoil is also known as the GA(W)–2 airfoil. Figure 3.17 shows a comparison of older NACA airfoils with the GA(W)–2 airfoil. Figure 3.17 also shows a comparison of the camber and thickness distributions for the GA(W)–1 airfoil with those for the NACA 65_3–018 airfoil. Several key design features of the 17% thick GA(W)–1 airfoil are:

Table 3.2 Examples of NACA Airfoil Designations

4-digit airfoils **Example: NACA 4412**

4	camber: 0.04c
4	position of the camber at 0.4c from the leading edge (L.E.)
12	maximum thickness: 0.12c

5-digit airfoils **Example: NACA 23015**

2	camber: 0.02c
	the design lift coefficient is 0.15 times the first digit for this series
30	position of the camber at (0.30/2) = 0.15c from the leading edge (L.E.)
15	maximum thickness: 0.15c

6-series airfoils **Example: NACA 65_3-421**

6	series designation
5	minimum pressure occurs at 0.5c
3	the drag coefficient is near its minimum value over a range of lift coefficients of 0.3 above and below the design lift coefficient
4	design lift coefficient is 0.4
21	maximum thickness: 0.21c

7-series airfoils **Example: NACA 747A315**

7	series designation
4	favorable pressure gradient on the upper surface from the L.E. to 0.4c at the design lift coefficient
7	favorable pressure gradient on the lower surface from the L.E. to 0.7c at the design lift coefficient
A	a serial letter to distinguish different sections having the same numerical designation but different mean line or different thickness distribution
3	design lift coefficient is 0.3
15	maximum thickness: 0.15c

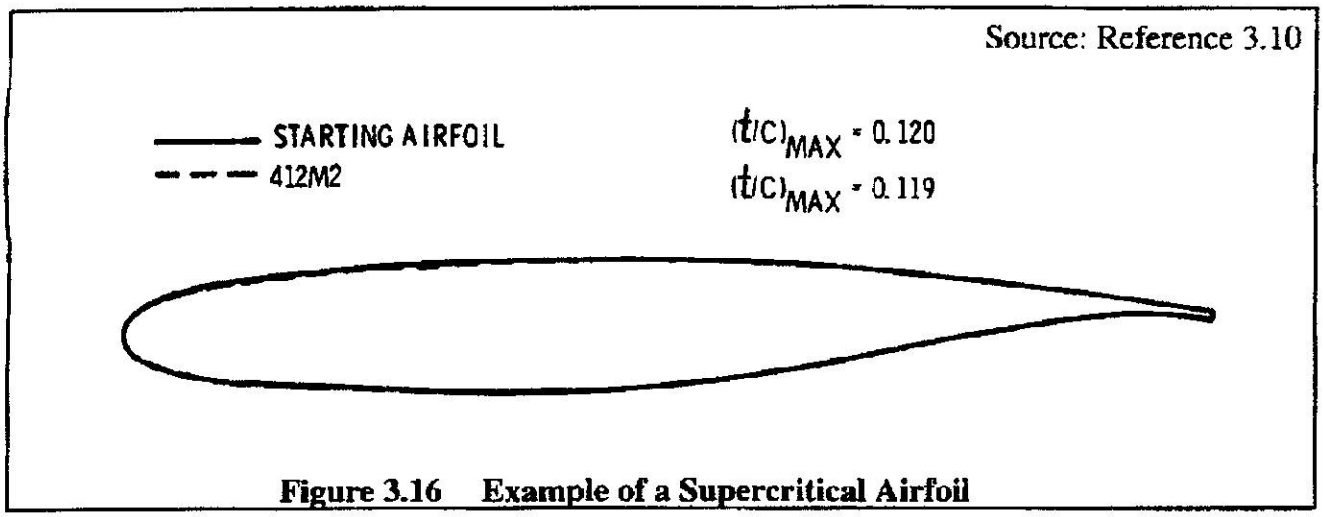

Figure 3.16 Example of a Supercritical Airfoil

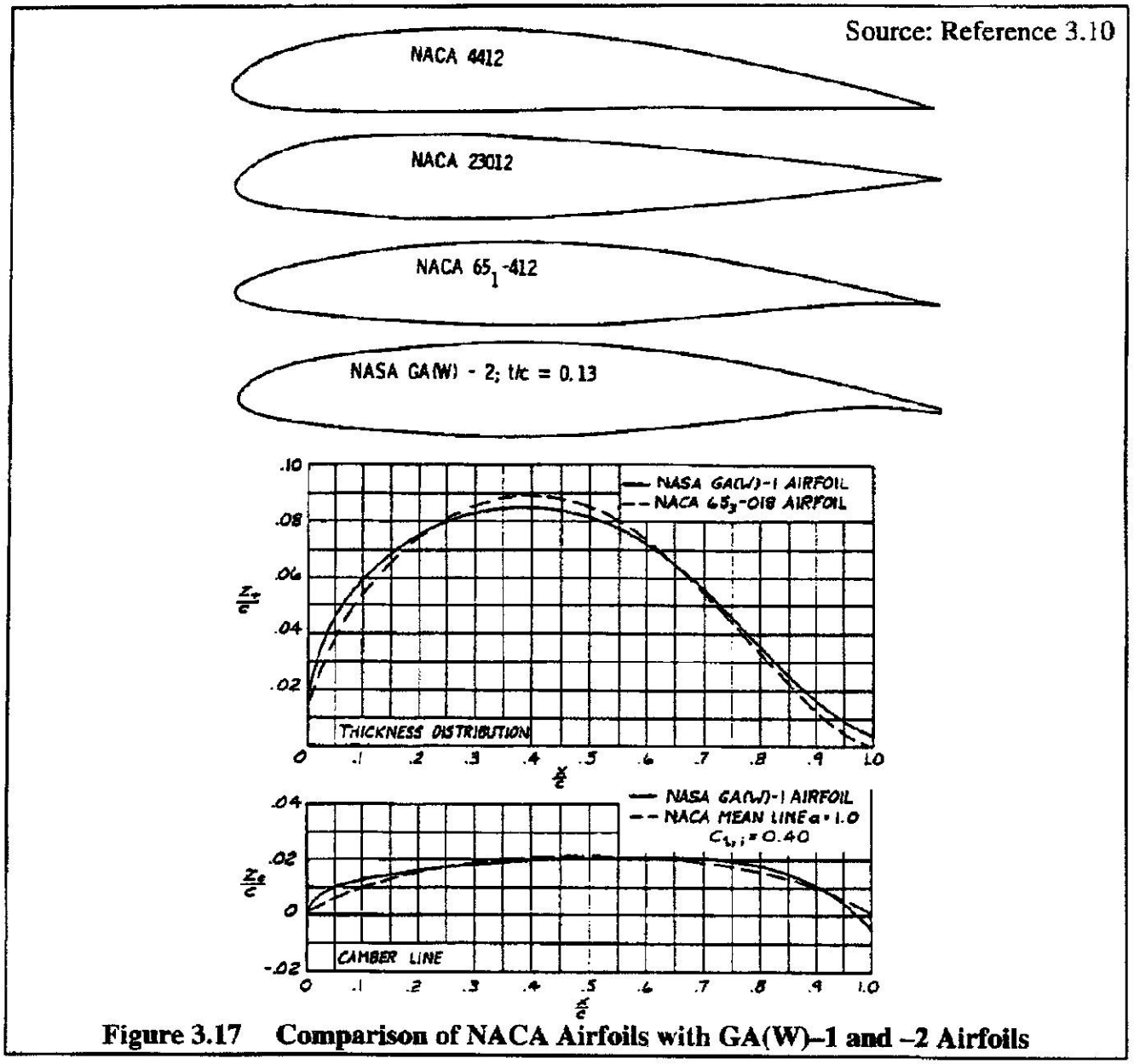

Figure 3.17 Comparison of NACA Airfoils with GA(W)–1 and –2 Airfoils

a) A large upper surface leading edge radius (0.06c) was used to alleviate the peak negative pressure coefficients and therefore delay airfoil stall to a higher angle of attack.

b) The airfoil was contoured to provide an approximate uniform chordwise load distribution near the design lift coefficient of 0.4.

c) A blunt trailing edge was provided with the upper and lower surface slopes approximately equal to moderate the upper surface pressure recovery and thus postpone the stall.

Test results in References 3.11 (for GA(W)-1) and 3.4 (for GA(W)-2) show that the section maximum lift coefficient, $c_{l_{max}}$ of this type airfoils is about 30% greater than that of a typical older NACA 6-series airfoil. This is achieved with a section lift-to-drag ratio, c_l/c_d at $c_l = 0.9$ which is about 50% greater! Figures 3.18a and 3.18b show some example data. In Figure 3.18b, the so-called NACA standard roughness is a large wrap-around roughness as compared with the narrow strip roughness strip now used as the NASA standard.

In selecting an airfoil for an airplane lifting surface (wing, canard, horizontal or vertical tail) the following considerations are important:

1) Drag (for example, one may wish to obtain the highest possible cruise speed)

2) Lift-to-drag ratio at values of the lift coefficient which are important to the airplane (for example, one may wish to design for a given climb rate with one engine inoperative)

3) Thickness (for example, one may wish to design the wing for a low structural weight)

4) Thickness distribution (for example, one may wish to design for a large internal fuel volume)

5) Stall characteristics (for example, one may wish to design for gentle stall characteristics)

6) Drag rise behavior (for example, one may wish to design for a high drag divergence Mach number. This item is closely linked to item 1).

7) Pitching moment characteristics (effect on trim drag)

It is clear from these seven items that airfoil design and/or airfoil selection will have to be done with a number of compromises in mind to achieve an acceptable overall result. Table 3.3 lists a number of practical airfoil applications.

Part VI of Reference 3.10 may be consulted for rapid, empirical methods to predict section lift, drag and pitching moment characteristics from the basic geometric parameters seen in Figure 3.14.

Source: Reference 3.10

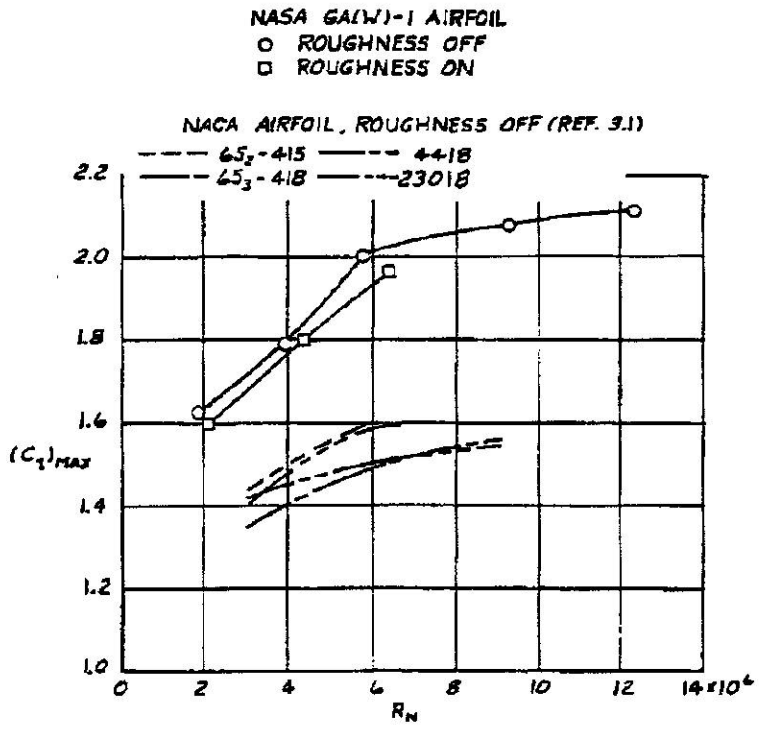

M = 0.15

a) Variation of Section Maximum Lift Coefficient with Reynolds Number

Source: Reference 3.10

$R_N = 6 \times 10^6$ and M = 0.2

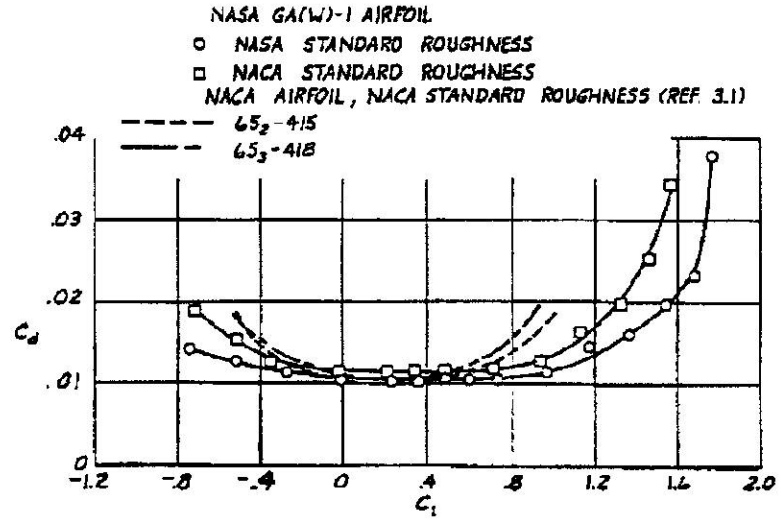

b) Variation of Section Drag Coefficient with Section Lift Coefficient

Figure 3.18 Comparison of Aerodynamic Characteristics of Some NACA and NASA Airfoils

Table 3.3 Examples of Airfoil Applications

Airplane Type	Wing	Horiz. Tail	Vert. Tail
Beech Bonanza	NACA 23016.5 (mod) at root NACA 23012 (mod) at tip –3° twist	NACA 0009	NACA 0009
Beech Queen Air B80	NACA 23020 (mod) at root NACA 23012 (mod) at tip –3° 54' twist	NACA 0009	NACA 0009
Beech Skipper	NASA GA(W)–1	NACA 0009	NACA 0009
Beech Duchess	NACA 63_2A415 (mod) at root	NACA 0009	NACA 0009
Cessna 210 Centurion	NACA 64_2A215 at root NACA 64_1A412 at tip –2° twist	NACA 0009	NACA 0009
Cessna T–37	NACA 2418 at root NACA 2412 at tip	NACA 0012	NACA 0012
Cessna 337 Skymaster	NACA 2412 at root NACA 2409 at tip –2° twist	NACA 0009	NACA 0009
Cessna 500 Citation	NACA 23014 (mod) at root NACA 23012 at tip –3° twist	NACA 0009	NACA 0009
Piper PA–23 Aztec	USA*35–B (mod) t/c = 14% –2.5° twist	NACA 0009	NACA 0009
Piper PA–31T Cheyenne	NACA $63_2$415 at root NACA 63 A212 at tip –2.5° twist	NACA 0009	NACA 0009
Lockheed 1329–25 Jetstar	NACA 63A112 at root NACA 63A309 at tip –2° twist	NACA 0009	NACA 0009
LTV A–7 Corsair	NACA 65A007	Not available	Not available
Northrop F–5A	NACA 65A004.8 (mod)	Not available	Not available
Boeing 747	Boeing proprietary airfoils. t/c=13.44% inboard t/c=7.8% mid–span t/c=8% tip	Not available	Not available

3.8 AIRFOIL MAXIMUM LIFT CHARACTERISTICS

The maximum lift characteristics of an airfoil as well as the associated stall behavior are of great importance to airplane performance.

Whenever the airflow around an airfoil separates, stall is said to have started. From a $c_l - \alpha$ viewpoint there are two types of stall: gradual and abrupt. Figure 3.19 shows examples of each type.

Source: Reference 3.10

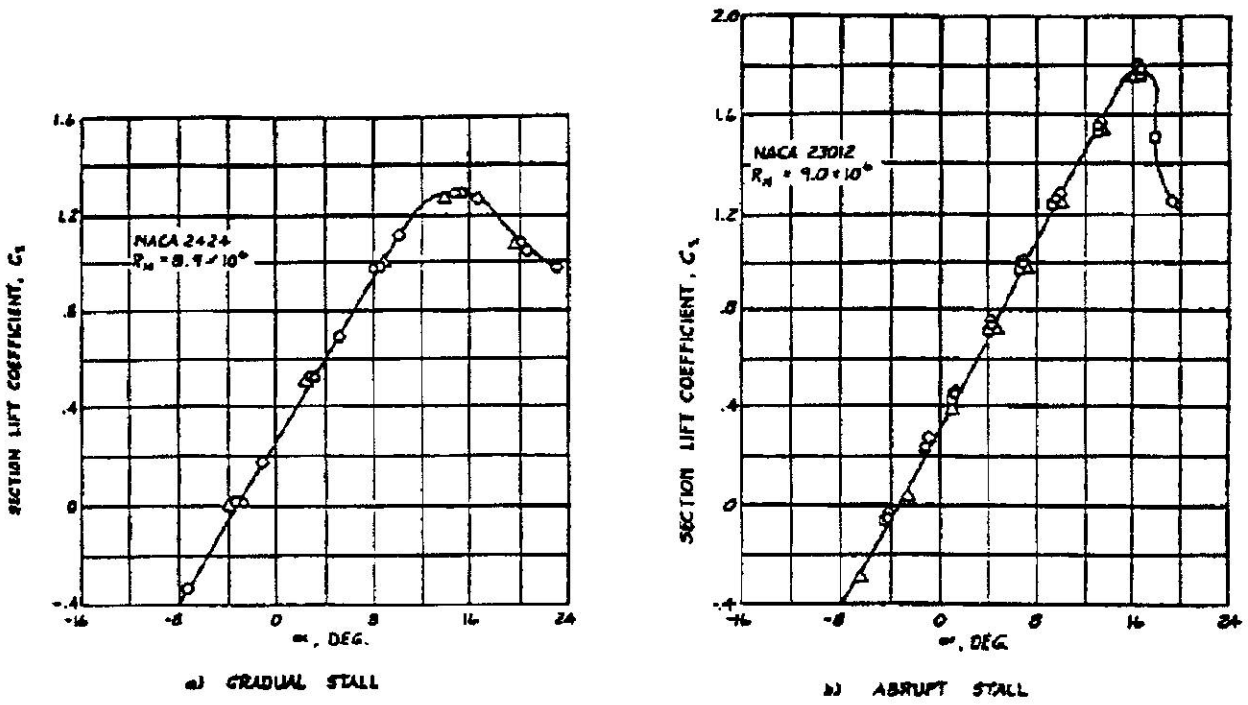

Figure 3.19 Example of Gradual and Abrupt Airfoil Stalls

The first type of stall is characterized by a gradual stall followed by a shallow drop–off of the section lift coefficient. This type of stall frequently occurs on airfoils with moderate or thick sections.

The second type of stall is characterized by an abrupt drop–off of the section lift coefficient. It is often associated with thin airfoil sections.

The main airfoil design features which affect section stall and therefore the maximum lift coefficient are:

a) thickness ratio
b) leading edge radius
c) camber
d) location of maximum thickness

These four factors are discussed in Sub–section 3.8.1.

3.8.1 GEOMETRIC FACTORS AFFECTING AIRFOIL MAXIMUM LIFT AT LOW SPEEDS

3.8.1.1 Thickness Ratio

Figure 3.20 shows how airfoil $c_{l_{max}}$ is affected by airfoil thickness ratio, t/c. It is shown in Sub–sub–section 3.8.1.2, that for a given thickness ratio, $c_{l_{max}}$ depends strongly on the leading edge radius and on the leading edge shape. Figure 3.20 also shows that the modern LS series of airfoils have considerably higher values of $c_{l_{max}}$ than conventional NACA airfoils. For the NACA airfoils, a thickness ratio of around 13% will generally produce the highest possible section lift coefficient. For the LS series of airfoils the highest vale of $c_{l_{max}}$ occurs at a thickness ratio of about 15%.

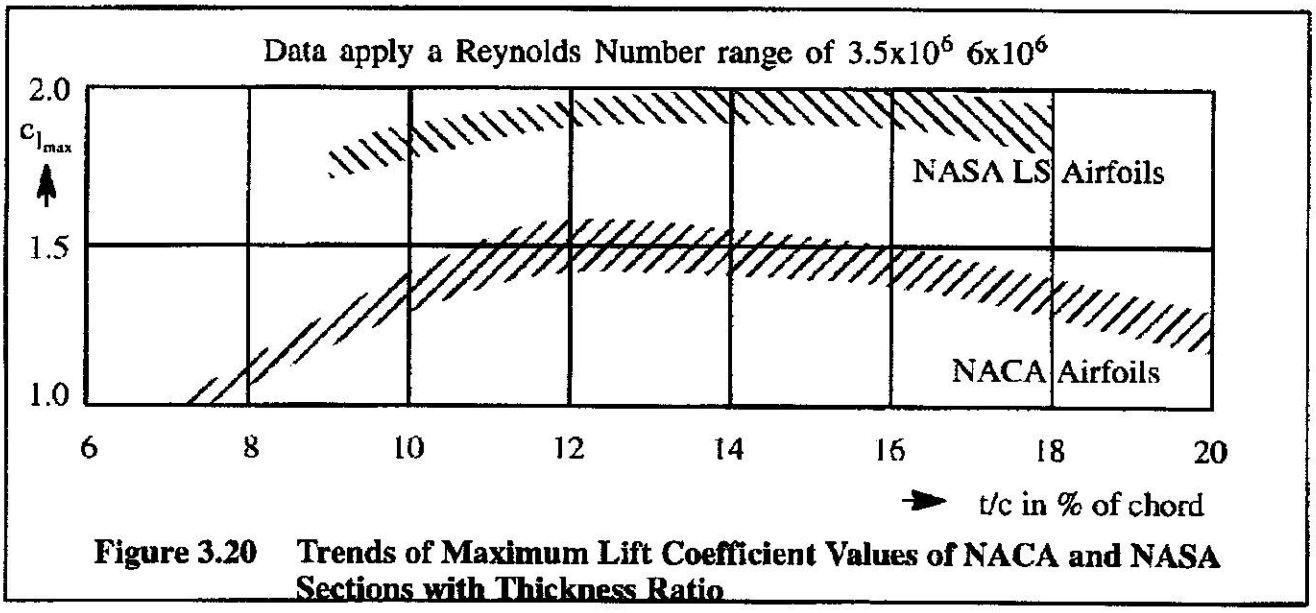

Figure 3.20 Trends of Maximum Lift Coefficient Values of NACA and NASA Sections with Thickness Ratio

3.8.1.2 Leading Edge Radius and Leading Edge Shape

The effect of leading edge radius and leading edge shape is more or less reflected in a geometric parameter, called: $\frac{z_5}{t}$, where z_5 is the local thickness of the airfoil at 5% chord and t is the maximum thickness of the airfoil. Figure 3.21 shows the effect of $\frac{z_5}{t}$ on section $c_{l_{max}}$ for NACA symmetrical airfoils of different thickness ratios. A large value of $\frac{z_5}{t}$ indicates a large leading edge radius. It is seen that large leading edge radii are beneficial in producing large values of $c_{l_{max}}$ at low speeds.

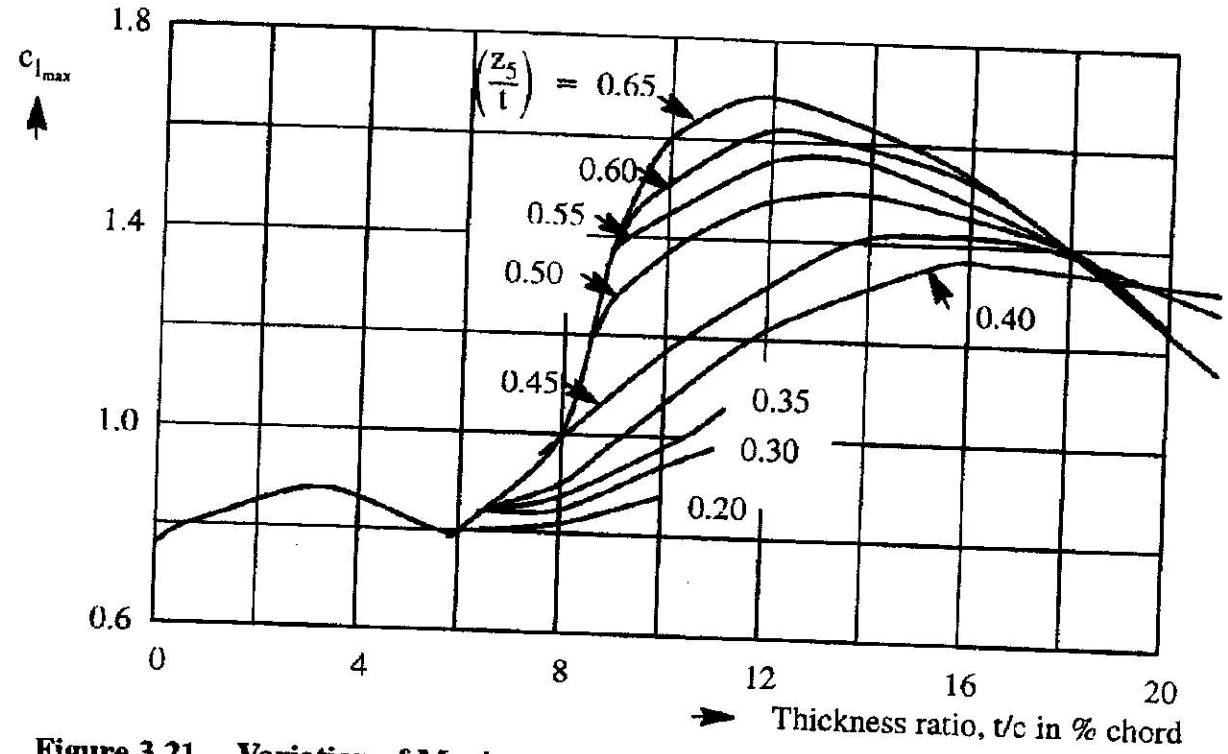

Figure 3.21 Variation of Maximum Lift Coefficient with Geometry of NACA Symmetrical Airfoils at a Reynolds Number of 6x10⁶

3.8.1.3 Camber and Location of Maximum Thickness

Experimental data show that the maximum lift coefficient of a cambered section depends not only on the amount of camber and camber line shape, but also on the thickness and nose radius of the section on which it is used.

In general, the addition of camber is always beneficial to $c_{l_{max}}$ and the benefit grows with increasing camber. The increment to maximum lift due to camber is least for sections with relatively large leading edge radii (i.e. the benefit of camber grows with reduction of the parameter $\frac{z_5}{t}$; and camber is more effective on thin sections than on thick sections.

In addition, a forward position of maximum camber produces higher values of $c_{l_{max}}$. For example, the NACA 23012 airfoil (with 2% maximum camber at 0.15 chord) has a $c_{l_{max}}$ of 1.79 as compared with 1.67 for NACA 4412 (with 4% camber at 0.4 chord but the same thickness distribution) at a Reynolds number of 9x106.

VELIVOLI - Profili e spessori percentuali

MONOMOTORE AD ELICA	corda alla radice [m]	profilo o spessore perc alla radice	profilo o spess perc all'estremità
Cessna Skyhawk		NACA 2412	NACA 2412
Cessna Skylane		2412	2412
Cessna Centurion		64A215	64A412
Cessna Crusader		23017	23012
Beechcraft		23016	23012
Piper Warrior		65-415	
BIMOTORI AD ELICA			
Beechcraft Kingair		23018	23011
Cessna Crusader		23017	23012
Cessna 402C		23018	23009
Piper Mojave		63-415	63-212
P68		63-3-515	63-3-515
TURBOELICA TRASP REG.			
ATR42		18%	13%
Fokker 50		64-421	64-415
VELIVOLI DA TRASP A GETTO			
DC10	10.71	12.2%	8.4%
A300	8÷9	10.5%	
B747	16.56	13.4%	8%
Fokker 100	5.3	12.3%	9.6%

Table A6.1 *Low-speed aerofoil section aerodynamic properties – NACA experimental data from Abbott and Von Doenhoff [44]*

Aerofoil	α_0 (deg)	C_{M_0}	$a_{1\text{rad}}$	$C_{l_{\alpha_{/\text{deg}}}}$	$\alpha_{C_{L_{max}}}$ (deg)	$C_{L_{max}}$	Section Cd at $C_{L_{max}}$
0006	0	0	6.19	0.108	9.0	0.92	0.0095
0009	0	0	6.25	0.109	13.4	1.32	0.0124
23012	−1.4	−0.014	6.13	0.107	18.0	1.79	0.016
23015	−1.0	−0.007	6.13	0.107	18.0	1.72	0.02
23018	−1.2	−0.005	5.96	0.104	16.0	1.60	0.016
23021	−1.2	0	5.90	0.103	15.0	1.50	0.0162
63–006	0	0.005	6.42	0.112	10.0	0.87	0.0086
63–009	0	0	6.36	0.111	11.0	1.15	0.0113
63–206	−1.9	−0.037	6.42	0.112	10.5	1.06	0.008
63–209	−1.4	−0.032	6.30	0.11	12.0	1.4	0.0127
63–210	−1.2	−0.035	6.47	0.113	14.5	1.56	0.014
63_1–012	0	0	6.65	0.116	14.0	1.45	0.0134
63_1–212	−2.0	−0.035	6.53	0.114	14.5	1.63	0.0117
63_1–412	−2.8	−0.075	6.70	0.117	15.0	1.77	0.0154
63A 010	0	0.005	6.02	0.105	13.0	1.2	0.0146
63A 210	−1.5	−0.04	5.9	0.103	14.0	1.43	0.014
64–006	0	0	6.25	0.109	9.0	0.8	0.007
64–009	0	0	6.3	0.11	11.0	1.17	0.0126
64–206	−1.0	−0.04	6.3	0.11	12.0	1.03	0.009
64–210	−1.6	−0.04	6.3	0.11	14.0	1.45	0.0118
64_1–412	−2.6	−0.065	6.42	0.112	15.0	1.67	–
64A 010	0	0	6.3	0.11	12.0	1.23	0.011
64A 210	−1.5	−0.04	6.02	0.105	13.0	1.44	0.011
64A 410	−3.0	−0.08	5.73	0.10	15.0	1.61	0.012
64_1A 212	−2.0	−0.04	5.73	0.10	14.0	1.54	0.012
64_2A 215	−2.0	−0.04	5.44	0.095	15.0	1.5	0.016
65–006	0	0	6.02	0.105	12.0	0.92	0.008
65–009	0	0	6.13	0.107	11.0	1.08	0.012
65–206	−1.6	−0.031	6.02	0.105	12.0	1.03	0.009
65–210	−1.6	−0.034	6.19	0.108	13.0	1.4	0.0137

$R_e = 9 \times 10^6$, smooth leading-edge.

The first integer indicates the maximum value of the mean-line ordinate y_c in per cent of the chord. The second integer indicates the distance from the leading edge to the location of the maximum camber in tenths of the chord. The last two integers indicate the section thickness in per cent of the chord. Thus the NACA 2415 wing section has 2% camber at 0.4 of the chord from the leading edge and is 15% thick.

Table A6.2 *Section aerodynamic properties – advanced*

Table A6.2 *Section aerodynamic properties – advanced aerofoil sections at high subsonic speeds*

Aerofoil	C_L	C_{Mo} at cruise	a_1/rad	$C_{L\alpha}$/deg	$c_{L_{max}}$ (Low speed)	Section Cd at given cruise C_L at M_D	t/c max	M drag rise at given C_L	Reference for data
RAE9515	0.3	−0.106	6.47	0.163	1.0	0.013	0.105	0.79	RAE R&M 3820, 1978 [45]
	0.4	−0.106	(Low Speed)			0.013		0.79	
	0.5	−0.11				0.013		0.79	
	0.6	−0.12				0.014		0.79	
RAE9530	0.3	−0.12	5.84	0.102	1.23	–	0.105	0.80	RAE R&M 3820, 1978 [45]
	0.4	−0.12	(Low Speed)			0.015		0.795	
	0.5	−0.13				0.015		0.79	
	0.6	−0.5				0.018		0.78	
RAE9550	0.3	−0.08	6.88	0.12	1.08		0.122	0.775	RAE R&M 3820, 1978 [45]
	0.4	−0.09						0.77	
	0.5	−0.095						0.765	
	0.6	−0.01						0.72	
RAE5225	0.3	−0.08			–	0.0107	0.14	–	RAE TR 87002 [46]
	0.4	−0.10			all at	0.0107		–	
	0.5	−0.1			M = 0.735	0.011		–	
RAE5230	0.6	−0.1				0.0114		0.735	RAE TR87002 [46]
	0.3	−0.1				0.0112	0.14	–	–
	0.4	−0.1			all at	0.0111		–	
	0.5	−0.1			M = 0.735	0.011			–
RAE5236	0.5	−0.1				0.012		0.735	RAE TR87002 [46]
	0.3	−0.076				0.0111	0.14		–
	0.4	−0.078			all at	0.0113			–
	0.5	−0.076			M = 0.735	0.0116			
	0.6	−0.076				0.0122		0.735*	
NACA SC(3)	0.3	−0.17			all at	0.0122	0.12		NASA TM–86371 [47]
−0712(B)	0.4	−0.18			M = 0.78	0.014			–
	0.5	−0.18			$R_e = 30 \times 10^6$	0.018			–
	0.6	−0.18				0.021		0.80**	
DSMA523	0.3	–			all at	0.012	0.11		NASA TM–81336 [48]
	0.4	–			M = 0.8	0.012			
	0.5	–			$R_e = 14.5 \times 10^6$	0.013			
	0.6	–				0.016		0.8	

* At $C_L = 0.58$ ** at $C_L = 0.68$.

Table 6.1 Homebuilt Airplanes: Wing Geometric Data

Type	Dihedral Angle, Γ_w, deg.	Incidence Angle, i_w, root/tip deg.	Aspect Ratio, A	Sweep Angle, $\Lambda_{c/4}$, deg.	Taper Ratio, λ_w	Max. Speed, V_{max}, kts	Wing Type
PIK-21 Duruble	0	0	3.8	0	1.0	NA	ctl/low
RD-03C PIEL	6.5	3/0	7.0	0	0.51	182	ctl/mid
CP-750	5.7	4.2	5.9	0	0.55	183	ctl/low
CP-90	5.7	3	5.4	0	0.44	171	ctl/low
POTTIER P-50R	4.4	NA	5.1	2	0.54	167	ctl/low
P-70S	0	2	4.8	0	1.0	129	ctl/mid
O-O Aerosport	2.5	NA	5.7	0	1.0	76	ctl/low
Aerocar Micro-Imp	0	4	4.7	0	1.0	260	ctl/high
Coats SA-III	4	1.5	5.6	0	1.0	165	ctl/low
Sequoia 300	3	3.5/1.5	6.9	0	0.55	243	ctl/low
Ord-Hume OH-4B	3	3	5	5.0	1.0	95	brcd/parasol
Procter Petrel	5	0	6.6	0	1.0	113	ctl/low
Bede BD-8	0	3	3.9	0	1.0	238	ctl/low

ctl = cantilever brcd = braced (strutted)

Table 6.2 Single Engine Propeller Driven Airplanes: Wing Geometric Data

Type	Dihedral Angle, Γ_w, deg.	Incidence Angle, i_w, root/tip deg.	Aspect Ratio, A	Sweep Angle, $\Lambda_{c/4}$, deg.	Taper Ratio, λ_w	Max. Speed, V_{max}, kts	Wing Type
CESSNA							
Skywagon 207	1.7	1.5/-1.5	7.4	0	0.69	182	brcd/high
Cardinal RG	1.5	4.1/0.7	7.3	0	0.73	156	ctl/high
Skylane RG	1.7	0.8/-2.8	7.4	0	0.67	187	brcd/high
PIPER							
Cherokee Lance	7.0	2/-1	6.2	0	1.0	188	ctl/low
Cher. Warrior	7.0	2/-1	7.2	5	0.67	152	ctl/low
Turbo Sarat.SP	6.8	NA	7.3	0	0.68	195	ctl/low
Bellanca							
Skyrocket	2	.2	6.7	0	0.57	287	ctl/low
Grumman Am.							
Tiger	5	1.4	7.1	0	1.0	148	ctl/low
Rockwell Commander							
112A	7	2	7.0	-2.5	0.50	180	ctl/low
Trago Mills							
SAB-1	5	3/1	7.5	0	0.54	202	ctl/low
Scottish Aviation							
Bullfinch	6.5	1.2	8.4	0	0.57	150	ctl/low
Robin HR100/4	6.3	4.7	5.4	0	1.0	180	ctl/low
Socata Rallye							
235E	7	4	7.6	0	1.0	148	ctl/low
Fuji FA-200	7	2.5	6.3	0	1.0	123	ctl/low
Gen Avia F15F	6	4	7.7	0	0.49	167	ctl/low

ctl = cantilever brcd = braced (strutted)

Table 6.3 Twin Engine Propeller Driven Airplanes: Wing Geometric Data

Type	Dihedral Angle, Γ_w, deg.	Incidence Angle, i_w, root/tip deg.	Aspect Ratio, A	Sweep Angle, $\Lambda_{c/4}$, deg.	Taper Ratio, λ_w	Max. Speed, V_{max}, kts	Wing Type
CESSNA							
310R	5	2.5/-.5	7.3	0	0.67	236	ctl/low
402B	5 (outer)	2/-.5	7.5	0 L.E.	0.67	227	ctl/low
414A	5	2.5/-.5	8.6	0 L.E.	0.60	232	ctl/low
T303	7	3/0	8.1	0 L.E.	0.71	216	ctl/low
PIPER							
PA-31P	6	1/-1.5	7.2	0	0.39	243	ctl/low
PA-44-180T	7.2	NA	8.1	0	0.63	196	ctl/low
Chieftain	5	1/-1.5	7.2	1.9	0.40	231	ctl/low
Cheyenne I	5	1.5/-1	7.4	0	0.37	249	ctl/low
Cheyenne III	5	1.5	7.8	0	0.31	296	ctl/low
BEECH							
Duchess 76	6.5	3/.6	8.0	0	0.80	194	ctl/low
Duke B60	6	4/0	7.2	0	0.32	246	ctl/low
Learfan 2100	4	1.5	9.5	0	0.45	369	ctl/low
Rockwell Commander 700	7	NA	9.0	0	0.43	231	ctl/low
Piaggio P166-DL3	21.5/2.5*	2.7	7.3	7.5	0.35	215	ctl/gull
EMB-121	7	3	7.2	0.33	0.61	316	ctl/low

ctl = cantilever brcd = braced (strutted)
*21.5 inboard, 2.5 outboard on this gull wing configuration

Table 6.4 Agricultural Airplanes: Wing Geometric Data

Type	Dihedral Angle, Γ_w, deg.	Incidence Angle, i_w, root/tip deg.	Aspect Ratio, A	Sweep Angle, $\Lambda_{c/4}$, deg.	Taper Ratio, λ_w	Max. Speed, V_{max}, kts	Wing Type
IAR-822	5 (outer)	5	6.3	0	1.0	92	ctl/low
UTVA-65	2	2.5	7.2	0	0.7	95	brcd/low
IA-53	7.5 (out)	4.3	6.3	0	0.7	116	ctl/low
EMB-200	7	3	7.0	0	1.0	116	ctl/low
Ag-cat	3	6	8.7	0	1.0	113	brcd/bipl
WSK M-15	NA	NA	NA	0	NA	146	brcd/bipl
PZL M-18A	1.3	3	7.8	0	1.0	128 138*	ctl/low
PZL 106A	4	6.5	7.8	4	1.0	114*	brcd/low
NDN-6	4.3	4.5	7.5	0	0.7	135	brcd/low
Cessna AgHusky	9	1.5/-1.5	8.5	0	0.7	106	brcd/low
Antonov AN-2M	2.5 both wings	NA	NA	0	1.0	136	brcd/bipl
HAL-31	6	0	6.0	0	1.0	108	ctl/low

*speed without spray equipment installed
ctl = cantilever brcd = braced (strutted) bipl = biplane

Table 6.5 Business Jets: Wing Geometric Data

Type	Dihedral Angle, Γ_w, deg.	Incidence Angle, i_w, root/tip deg.	Aspect Ratio, A	Sweep Angle, $\Lambda_{c/4}$, deg.	Taper Ratio, λ_w	Max. Speed, V_{max}, kts	Wing Type
DASSAULT/BREGUET							
Falcon 10	1.5	NA	7.1	27	0.36	492(25K)	ctl/low
Falcon 20F	2	1.5	6.4	30	0.31	465(25K)	ctl/low
Falcon 50	0	NA	7.6	24	0.32	475	ctl/low
CESSNA							
Citation I 500	4	2.5/-0.5	7.8	0	0.39	277(28K)	ctl/low
Citation II	4.7	NA	8.3	2	0.32	277(28K)	ctl/low
Citation III	2.8	NA	8.9	25	0.35	472(33K)	ctl/low
GATES LEARJET							
24	2.5	1	5.0	13	0.50	473(31K)	ctl/low
35A	2.5	1	5.7	13	0.50	464	ctl/low
55	2.9	NA	7.3	13	0.42	470(30K)	ctl/low
IAI							
1124 Westw. I	2	1/-1	6.5	5	0.33	471	ctl/mid
1125 Astra	2.6 (out)	NA	8.8	34/25 at LE	0.30	472(35K)	ctl/low
Canadair CL601	2.3	3	8.5	25	0.26	450	ctl/low
BAe 125-700	2	2.1/-0.3	6.3	20	0.28	436(28K)	ctl/low
GA Gulfst. III	3	3.5/-0.5	6.5	28	0.31	487	ctl/low
Mu Diamond I	2.7	3/-3.5	7.5	20	0.35	431(30K)	ctl/low
L. Jetstar II	2	1/-1	5.3	30	0.37	475(30K)	ctl/low

ctl = cantilever (30K) = 30,000 ft altitude

Table 6.6 Regional Turbopropeller Driven Airplanes: Wing Geometric Data

Type	Dihedral Angle, Γ_w, deg.	Incidence Angle, i_w, root/tip deg.	Aspect Ratio, A	Sweep Angle, $\Lambda_{c/4}$, deg.	Taper Ratio, λ_w	Max. Speed, V_{max}, kts	Wing Type
CASA C-212-200							
SHORTS							
330	3 (outer)	NA	12.3	0	1.0	190(10K)	brcd/high
360							
BEECH							
1900	6	3.5/-1.1	9.8	0	0.42	263(8K)	ctl/low
B99	7	4.8	7.5	0	0.5	247(12K)	ctl/low
CESSNA CONQUEST							
I							
II							
GA Gulfstr. Ic							
GAF N22B							
Fokker F27-200	2.5	3.5	12.0	0	0.41	259(20K)	ctl/high
DeHAVILLAND CANADA							
DHC-6-300							
DHC-7	4.5	3	10.0	0	0.44	231(8K)	ctl/high
DHC-8	2.5 (out)	NA	12.3	0	0.45	270(15K)	ctl/high
EMB 110	7	3	9.9	0	0.50	248(8K))	ctl/low
EMB 120	6.5	2	9.9	0	0.50	NA	ctl/low
BRITISH AEROSPACE							
Jetstream 31	7	2	10.0	0.5	0.37	263(20K)	ctl/low
748	7	3	12.7	2.9	0.36	244(15K)	ctl/low

ctl = cantilever (30K) = 30,000 ft altitude

Table 6.7 Jet Transports: Wing Geometric Data

Type	Dihedral Angle, Γ_w, deg.	Incidence Angle, i_w, root/tip deg.	Aspect Ratio, A	Sweep Angle, $\Lambda_{c/4}$, deg.	Taper Ratio, λ_w	Max. Speed, V_{max}, kts	Wing Type
BOEING							
727-200	3	2	7.1	32	0.30	549(22K)	ctl/low
737-200	6	1	8.8	25	0.34	462(33K)	ctl/low
737-300	6	1	8.0	25	0.28	462(33K)	ctl/low
747-200B	7	2	7.0	37.5	0.25	523(30K)	ctl/low
747SP	7	2	7.0	37.5	0.25	529(30K)	ctl/low
757-200	5	3.2	7.9	25	0.26		ctl/low
767-200	6	4.3	7.9	31.5	0.27		ctl/low
McDONNELL DOUGLAS							
DC-9 Super 80	3	1.3	9.6	24.5	0.16	500	ctl/low
DC-9-50	1.5	NA	8.7	24	0.18	537	ctl/low
DC-10-30	5.3/3	+/-	7.5	35	0.25	530(25K)	ctl/low
AIRBUS							
A300-B4	5	NA	7.7	28	0.35	492(25K)	ctl/low
A310	11.1/4.1	5.3	8.8	28	0.26	483(30K)	ctl/low
Lockh.1011-500	7.5/5.5	NA	7.0	35	0.30	525(30K)	ctl/low
Fkr F28-4000	2.5	NA	8.0	16	0.31	390	ctl/low
Rombac 111-495	2	2.5	8.5	20	0.32	470(21K)	ctl/low
BAe 146-200	-3	3.1/0	9.0	15	0.36	420(26K)	ctl/high
Tupolev Tu154	0	NA	7.0	35	0.27	526(31K)	ctl/low

ctl = cantilever (30K) = 30,000 ft altitude

Table 6.8 Military Trainers: Wing Geometric Data

Type	Dihedral Angle, Γ_w, deg.	Incidence Angle, i_w, root/tip deg.	Aspect Ratio, A	Sweep Angle, $\Lambda_{c/4}$, deg.	Taper Ratio, λ_w	Max. Speed, V_{max}, kts	Wing Type
Propeller Driven							
EMB-312 Tucano	5.5	1.4/-0.8	6.4	0.7	0.47	292	ctl/low
Pilatus PC-7	7 (outer)	NA	6.5	1	0.55	270	ctl/low
NDN-1	5 (outer)	3	5.4	0	0.79	247	ctl/low
Beech T-34C	7	4/1	6.2	0	0.41	280	ctl/low
Aerosp.Epsilon	5	2	7.0	0	0.63	281	ctl/low
SM SF-260M	6.3	2.8/0	6.3	0	0.49	235	ctl/low
Yak-52	2	2	5.8	0	0.54	194	ctl/low
Neiva T-25	6	2	7.1	0	0.54	269	ctl/low
Jet Driven							
Aero L-39C	2.5	2	4.4	2	0.52	491	ctl/low
Microjet 200B	5	3	8	0	0.39	300	ctl/low
DB/D Alphajet	-6	NA	4.8	28	0.36	495(33K)	ctl/shldr
Aermac. MB339A	2.6	NA	5.3	9	0.58	500	ctl/low
SM S-211	-2	2.2/-1.3	5.1	16	0.46	400	ctl/shldr
PZL TS-11	2.7	NA	5.7	7	0.51	404	ctl/mid
CASA C-1-1	5	1	5.6	2	0.60	428(25K)	ctl/low
Bae Bawk Mk1	2	NA	5.3	22	0.34	572	ctl/low
Tupolev Tu154	0	NA	7.0	35	0.27	526(31K)	ctl/low

ctl = cantilever shldr = shoulder (30K) = 30,000 ft altitude

Table 6.9 Fighters: Wing Geometric Data

Type	Dihedral Angle, Γ_w, deg.	Incidence Angle, i_w, root/tip deg.	Aspect Ratio, A	Sweep Angle, $\Lambda_{c/4}$, deg.	Taper Ratio, λ_w	Max. Speed, V_{max}, kts	Wing Type
DASSAULT BREGUET							
Mirage III-E	-1	0	1.9	61(LE)	0	1,268(39K)	ctl/low
Mirage F1-C	-4.5	NA	2.8	48(LE)	0.29	1,260	ctl/shldr
Mirage 2000	-1	NA	2.0	58(LE)	0	1,260	ctl/low
Super Etendard	-3.5	NA	3.2	45	0.50	573	ctl/mid
Fairch.R.A-10A	7 (outer)	-1	6.5	0	0.66	450	ctl/low
Grumman A-6E	0	NA	5.3	25	0.30	700	ctl/mid
Grumman F14A	-1.5(out)	NA	7.3*	20/68(LE)	0.40	M = 2.4	vsw/high
Northrop F-5E	0	0	3.8	24	0.19	710	ctl/low
Vought A-7E	-5	-1	4	35	0.25	595(5K)	ctl/high
McDONNELL DOUGLAS							
F-4E	0/12	NA	2.8	45(LE)	0.18	1,146	ctl/low
F-15	-1	0	3.0	39	0.25	M =2.5	ctl/high
AV-8B	-12	1.8	4.0	24	0.28	585(0K)	ctl/shldr
GD FB-111A	0	NA	7.6*	16/73(LE)	0.33	1,260	ctl/shldr
GD F-16	0	0	3.0	40(LE)	0.22	495(33K)	ctl/mid
Cessna A37B	3	3.6/1	6.2	0	0.68	455	ctl/low
Aerm. MB339K	2.6	NA	5.3	8.5	0.58	500	ctl/low
Sukhoi Su-7BMK	0	NA	2.6	62(LE)	0.26	730(0K)	ctl/mid

ctl = cantilever shldr = shoulder (30K) = 30,000 ft altitude
* taken at lowest sweep angle

Table 6.10 Military Patrol, Bomb and Transport Airplanes: Wing Geometric Data

Type	Dihedral Angle, Γ_w, deg.	Incidence Angle, i_w, root/tip deg.	Aspect Ratio, A	Sweep Angle, $\Lambda_{c/4}$, deg.	Taper Ratio, λ_w	Max. Speed, V_{max}, kts	Wing Type
Turbopropeller Driven							
Lockh'd C130E	2.5	3/0	10.1	0	0.49	325	ctl/high
Lockheed P3C	6	0/0.5	7.5	0	0.40	411(15K)	ctl/low
Antonov 12BP	-3.8(out)	NA	11.9	7.4	0.34	419	ctl/high
Antonov 22	-3.5	NA	12.0	3	0.36	399	ctl/high
Antonov 26	-2(out)	3	11.7	7	0.34	NA	ctl/high
Grumman E2C	3.1	NA	9.3	5.3	0.34	325	ctl/high
DB Atlantic 2	6 (outer)	3	11.6	9 (LE)	0.39	348	ctl/low
Aerital.G222	2.5 (out)	NA	9.2	2.1	0.50	291	ctl/high
Transall C-160	3.5 (out)	NA	10.0	1.9	0.50	320	ctl/high
Jet Driven							
Lockheed S3A	0	3/-3.5	7.9	15	0.25	450	ctl/high
Lockh'd C-141B	-3.5	NA	7.5	25.5	0.41	492	ctl/high
Lockheed C-5A	-5.1	NA	7.8	25.6	0.34	496(25K)	ctl/high
BAe Nimrod Mk2	2.7	NA	6.2	20	0.23	500	ctl/low
Boeing YC-14	0	NA	9.4	4.6	0.30	438	ctl/high
McDD KC-10A	5/3	+/-	7.5	35	0.25	530(25K)	ctl/low
Tupolev Tu-16	-3.7	NA	6.6	43(LE)	0.44	535(6K)	ctl/high
Tupolev Tu-22	0	NA	4.0	51(LE)	0.31	800(40K)	ctl/mid
Ilyushin Il76T	-3.6	NA	11.7	25	0.37	459	ctl/high

ctl = cantilever shldr = shoulder (30K) = 30,000 ft altitude

Although the possibility of such airfoils was known for some time, their successful development in modern times is attributed to R. T. Whitcomb. A Whitcomb-type supercritical airfoil is pictured in Figure 3.7.

Tested at low speeds, the supercritical airfoils were found to have good $C_{l_{max}}$ values as well as low C_d values at moderate lift coefficients. As a result, another family of airfoils evolved from the supercritical airfoils, but for low-speed applications. These are the "general aviation" airfoils, designated GA(W) for general aviation (Whitcomb). The GA(W)-1 airfoil is the last of the

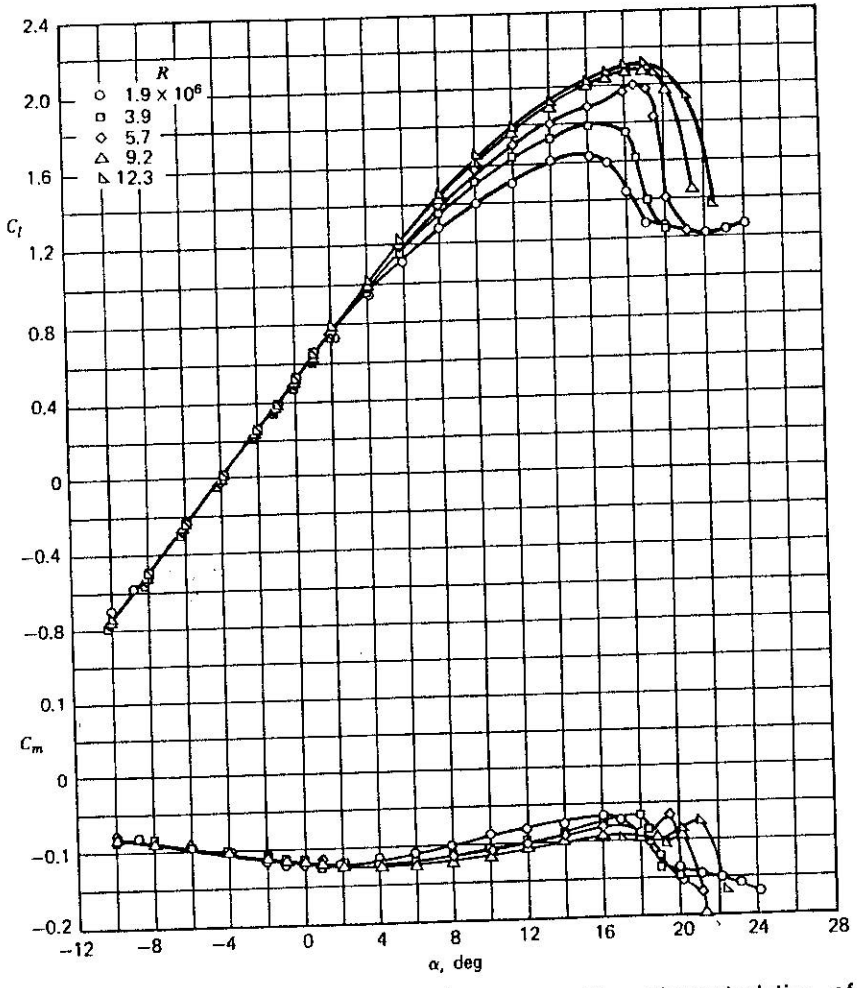

Figure 3.10a Effect of Reynolds number on section characteristics of the GA(W)-1 airfoil. Model smooth, $M = 0.15$.

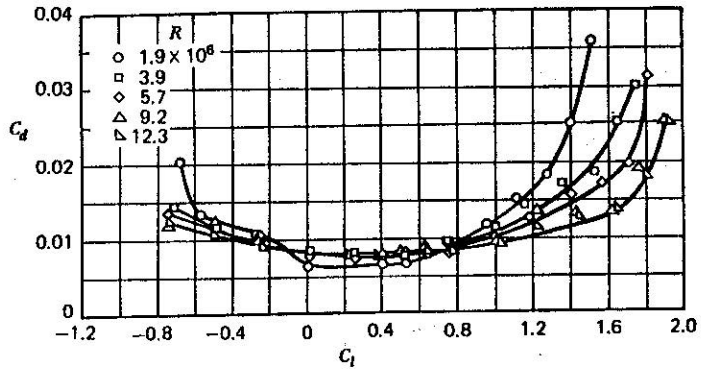

Figure 3.10b Conditions same as Figure 3.10a.

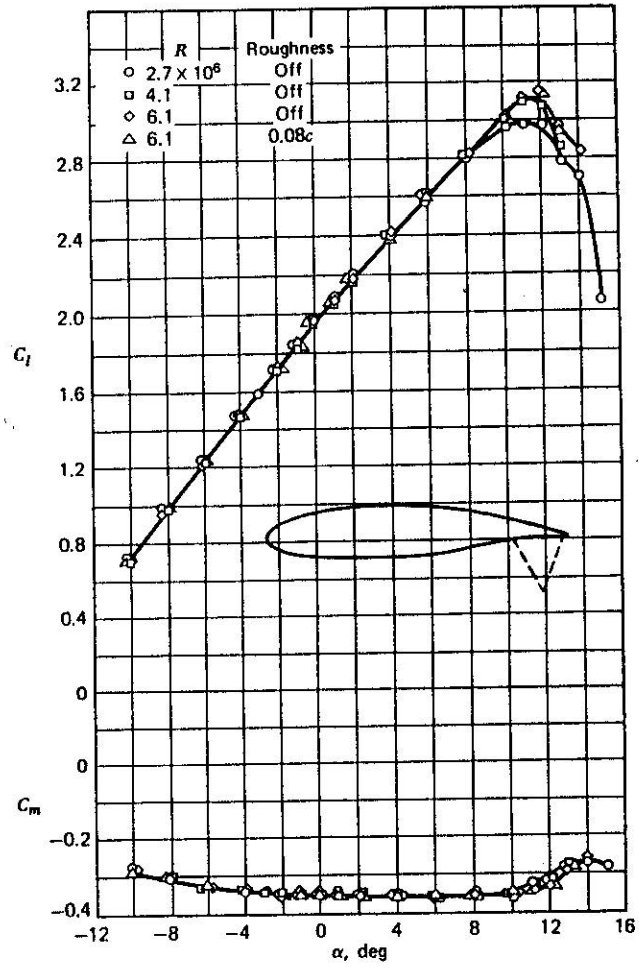

Figure 3.10c GA(W)-1 airfoil section characteristics for 0.20c simulated split flap

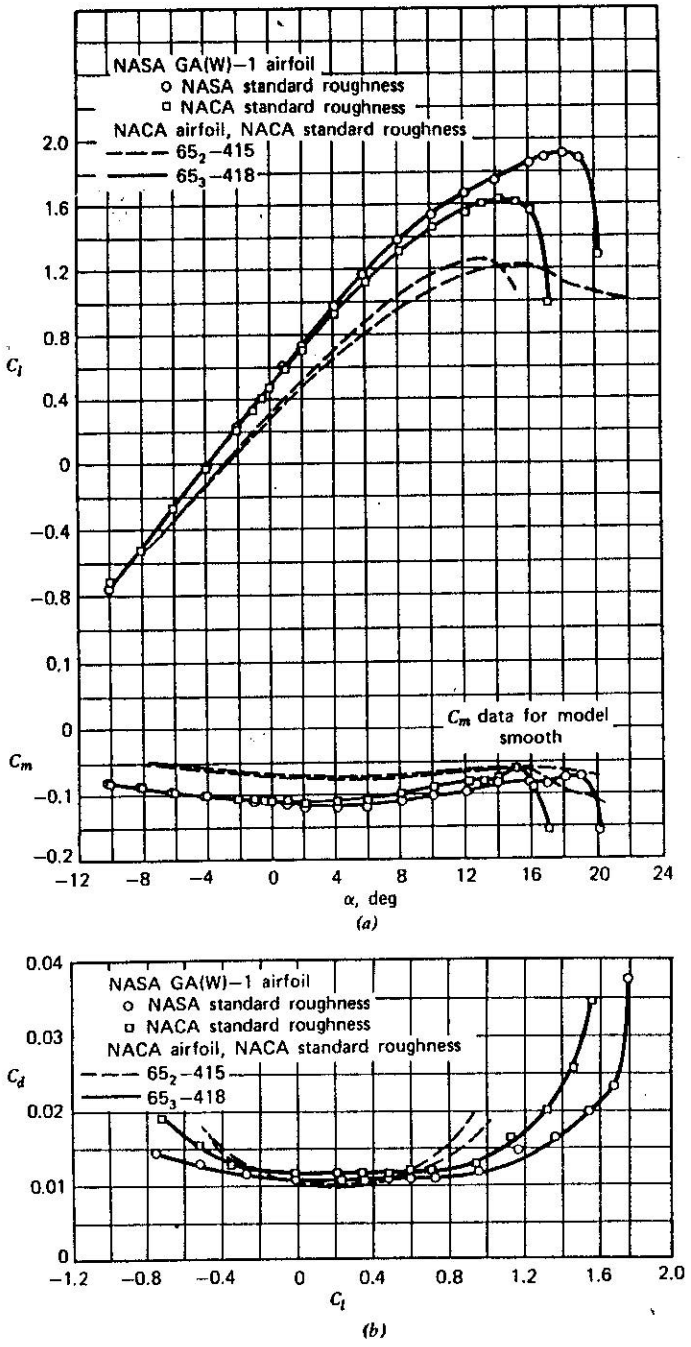

Figure 3.11 Comparison of section characteristics of NASA GA(W)-1 airfoil and NACA 65–415 and 65–418 airfoils. $M = 0.20$; $R \approx 6 \times 10^6$. (a) Variation of C_l and C_m with α. (b) Variation of C_d with C_l.

airfoils pictured in Figure 3.7. Test results for this airfoil are reported in Reference 3.8, where its $C_{l_{max}}$ values are shown to be about 30% higher than those for the older NACA 65-series airfoils. In addition, above C_l values of around 0.6, its drag is lower than the older laminar flow series with standard roughness. These data are presented in Figure 3.10 for the GA(W)-1 airfoil. Comparisons of $C_{l_{max}}$ and C_d for this airfoil with similar coefficients for other airfoils are presented in Figures 3.11 and 3.12.

Observe that the performance of the GA(W)-1 airfoil is very Reynolds number-dependent, particularly $C_{l_{max}}$, which increases rapidly with Reynolds number from 2 to 6 million. At the time of this writing, the GA(W) airfoil is beginning to be employed on production aircraft. The same is true of the supercritical airfoil. Indeed, the supercritical airfoil is being used on both the Boeing YC-14 and McDonnell-Douglas YC-15 prototypes currently being tested for the advanced medium STOL transport (AMST) competition. At the time of this writing, NASA is adopting a new nomenclature for the GA(W) airfoils. They will be designated by LS (low speed) or MS (medium speed) followed by four digits. For example, the GA(W)-1 airfoil becomes LS(1)-0417. The (1) designates a family. The 04 refers to a design lift coefficient of 0.4, and 17 is the maximum

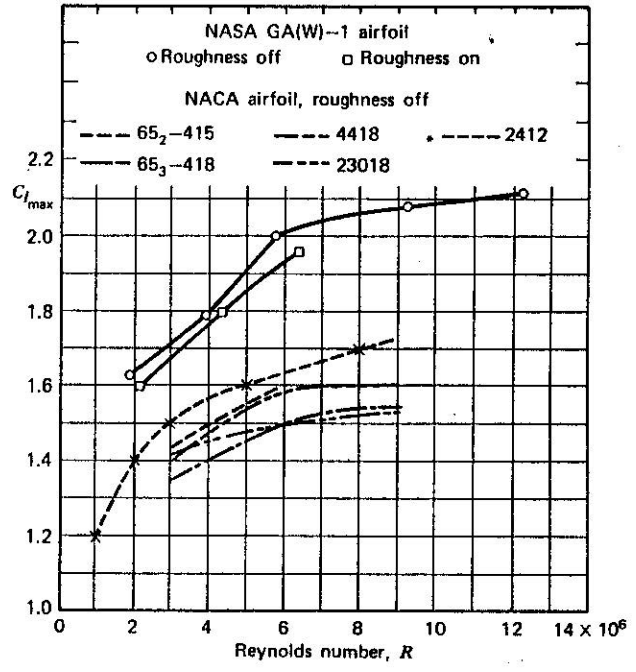

Figure 3.12 Comparison of maximum lift coefficient of the GA(W)-1 airfoil with other NACA airfoils $M = 0.15$.

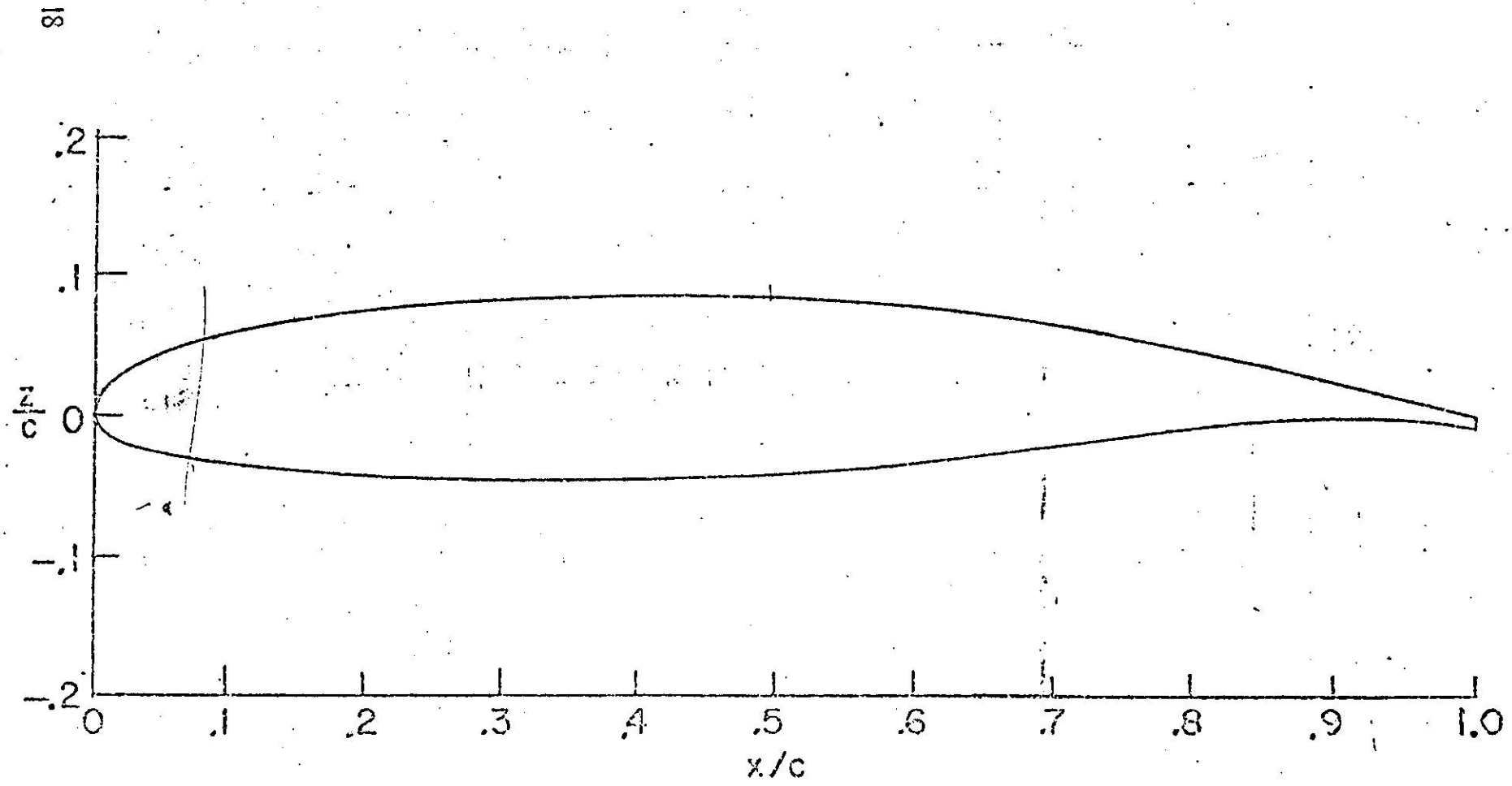

Figure 1. - Section shape for NASA GA(W)-2 airfoil.

GA(W)-2. t/c = 0.13

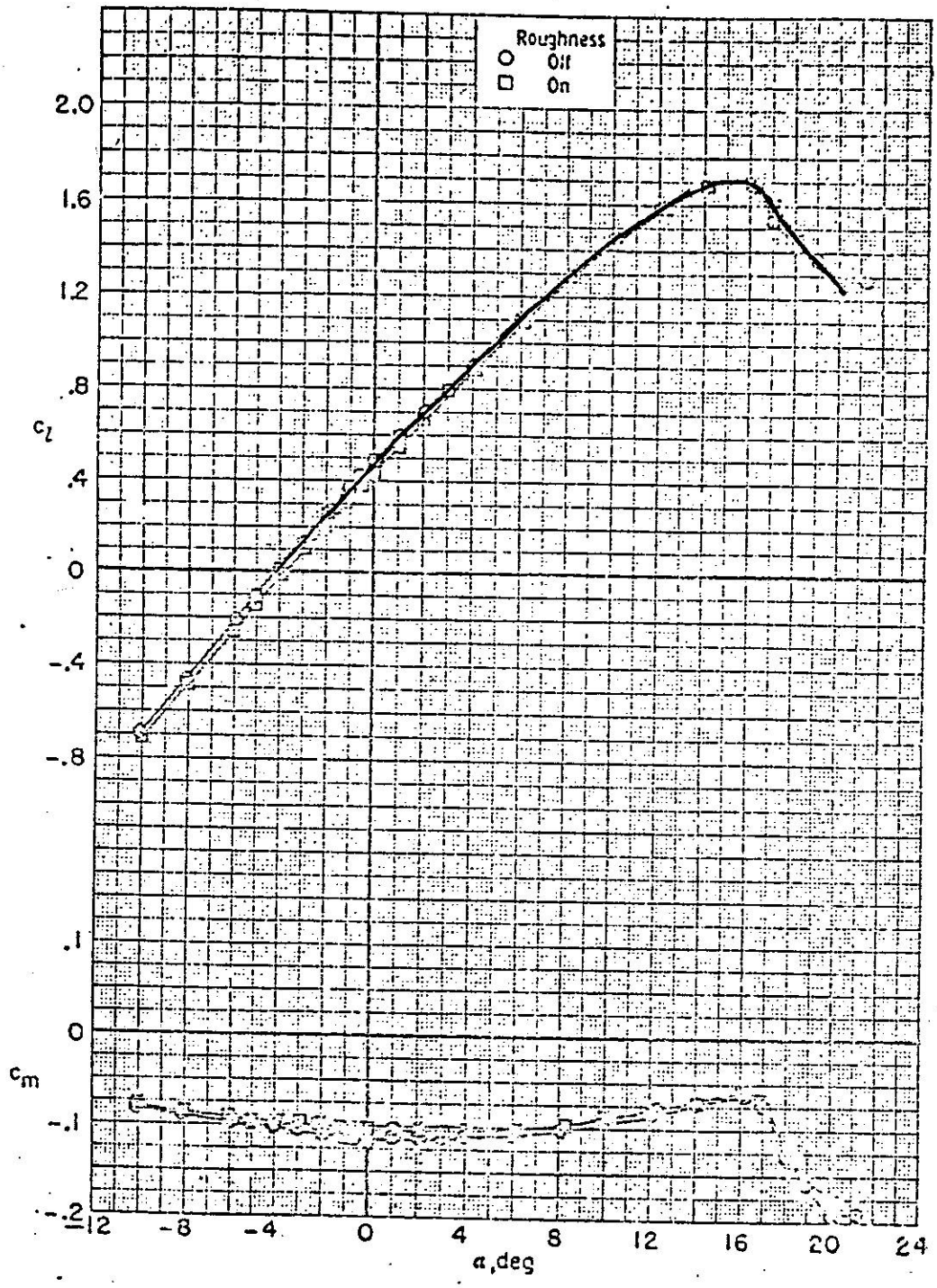

(a) $R = 2.1 \times 10^6$.

Figure 6.- Effect of Reynolds number on airfoil section characteristics. M = 0.15.

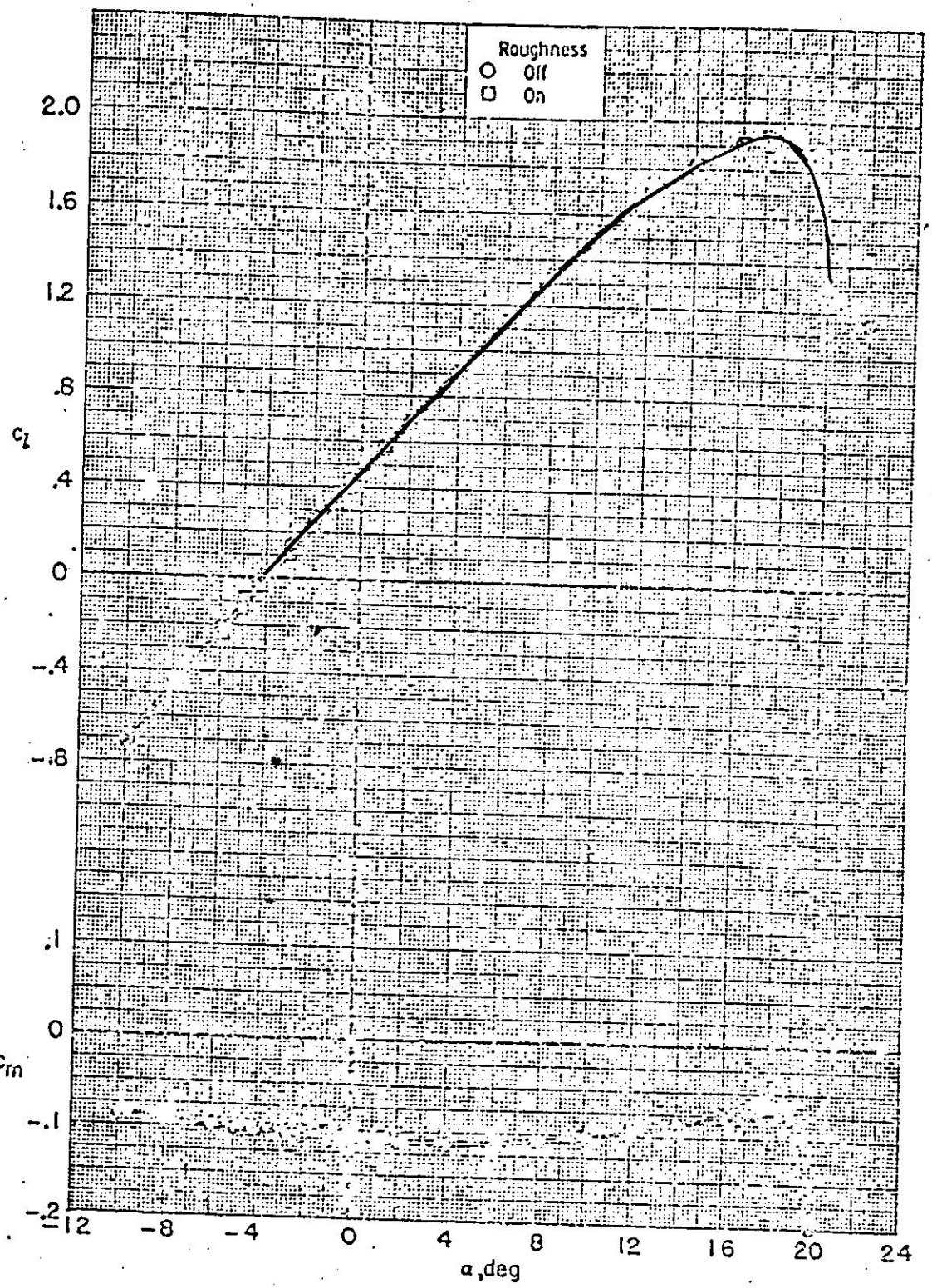

(c) $R = 4.1 \times 10^6$.

Figure 6.- Continued.

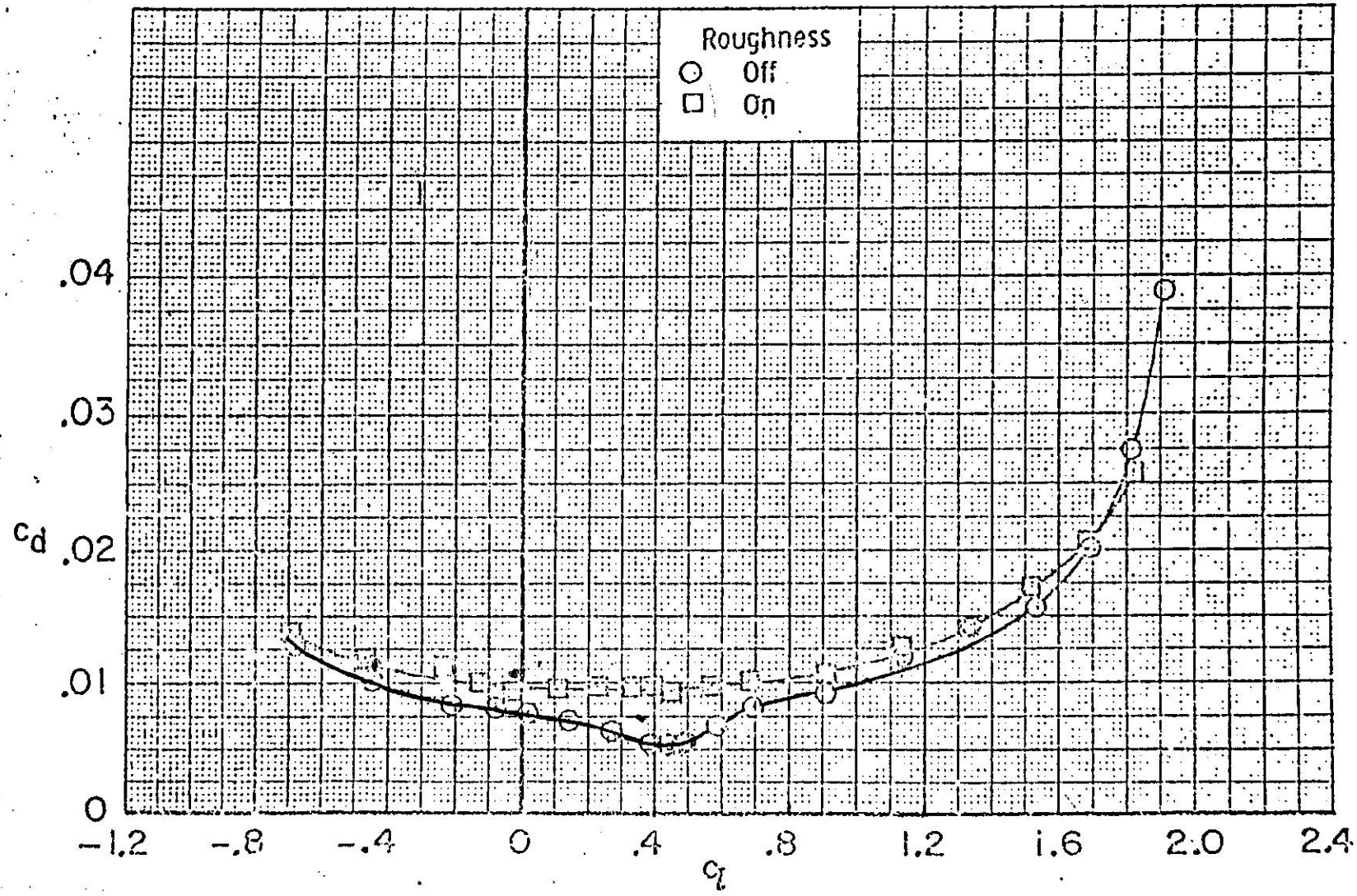

(c) $R = 4.1 \times 10^6$. Concluded.

Figure 6. - Continued.

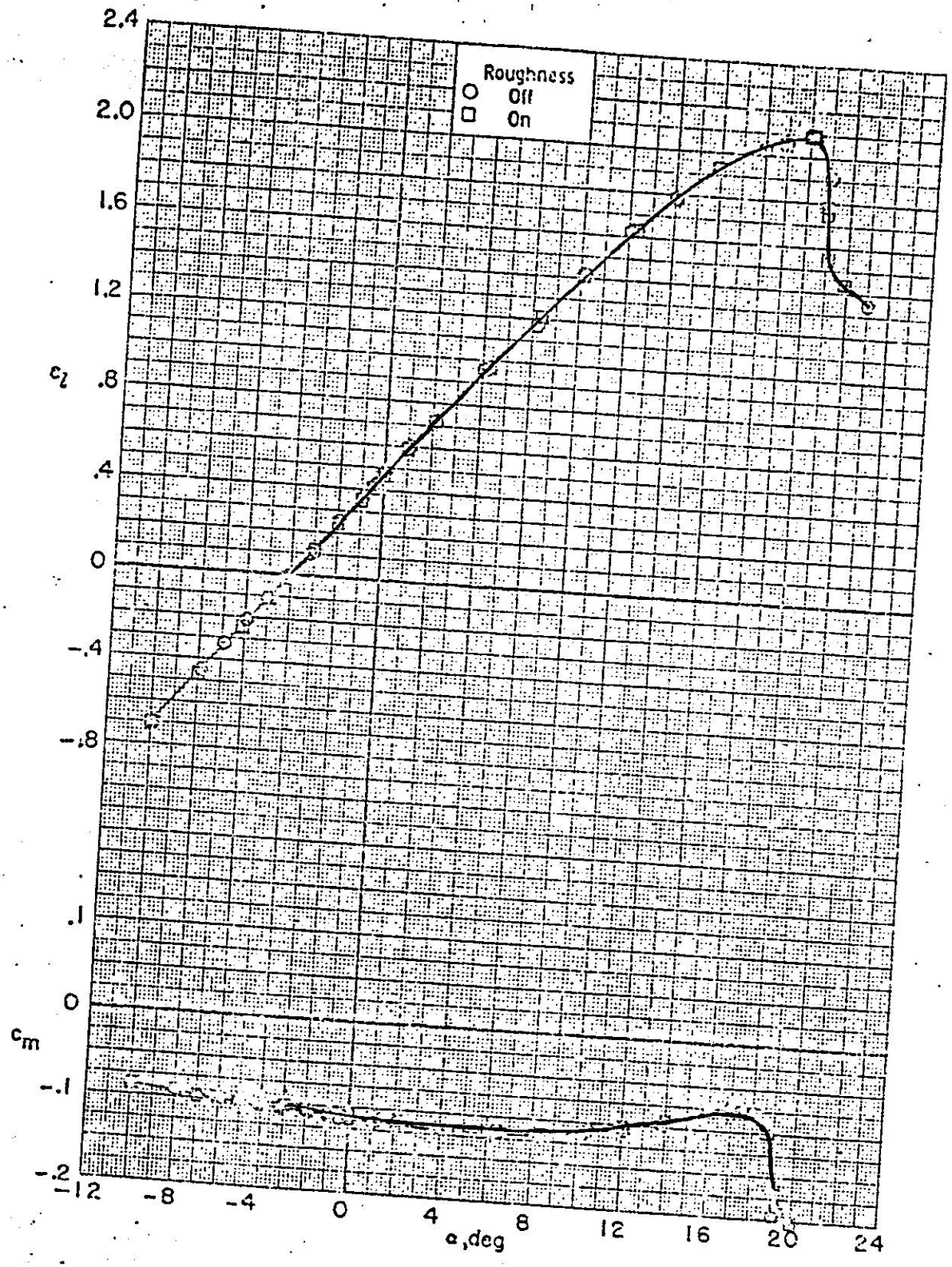

(e) $R = 9.4 \times 10^6$.

Figure 6. - Continued.

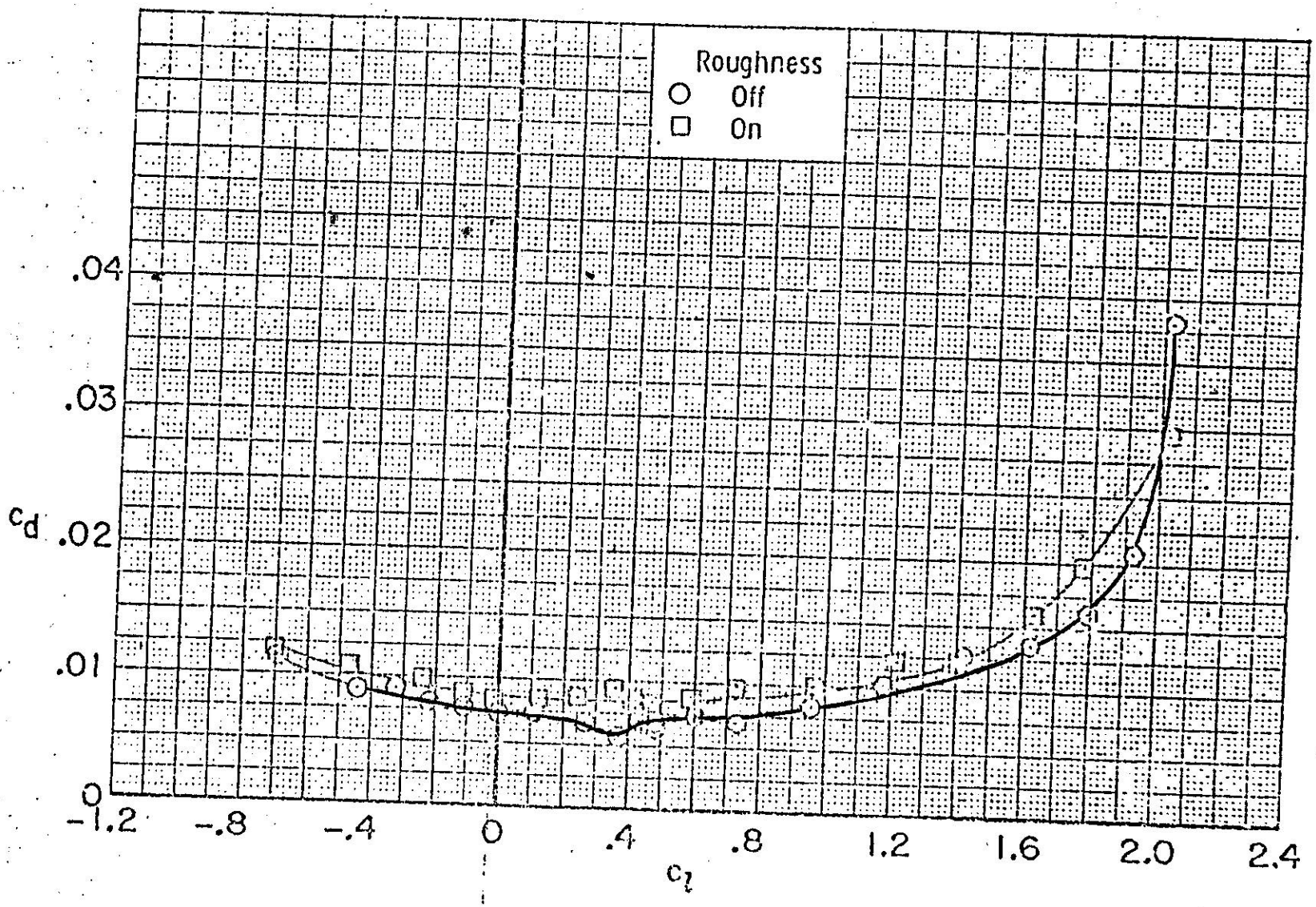

(e) R = 9.4 x 10^6. Concluded.

Figure 6.- Concluded.

17

NOTE: FOR SUPERCRITICAL AIRFOILS USE $\Delta M_{CR} = 0.05$

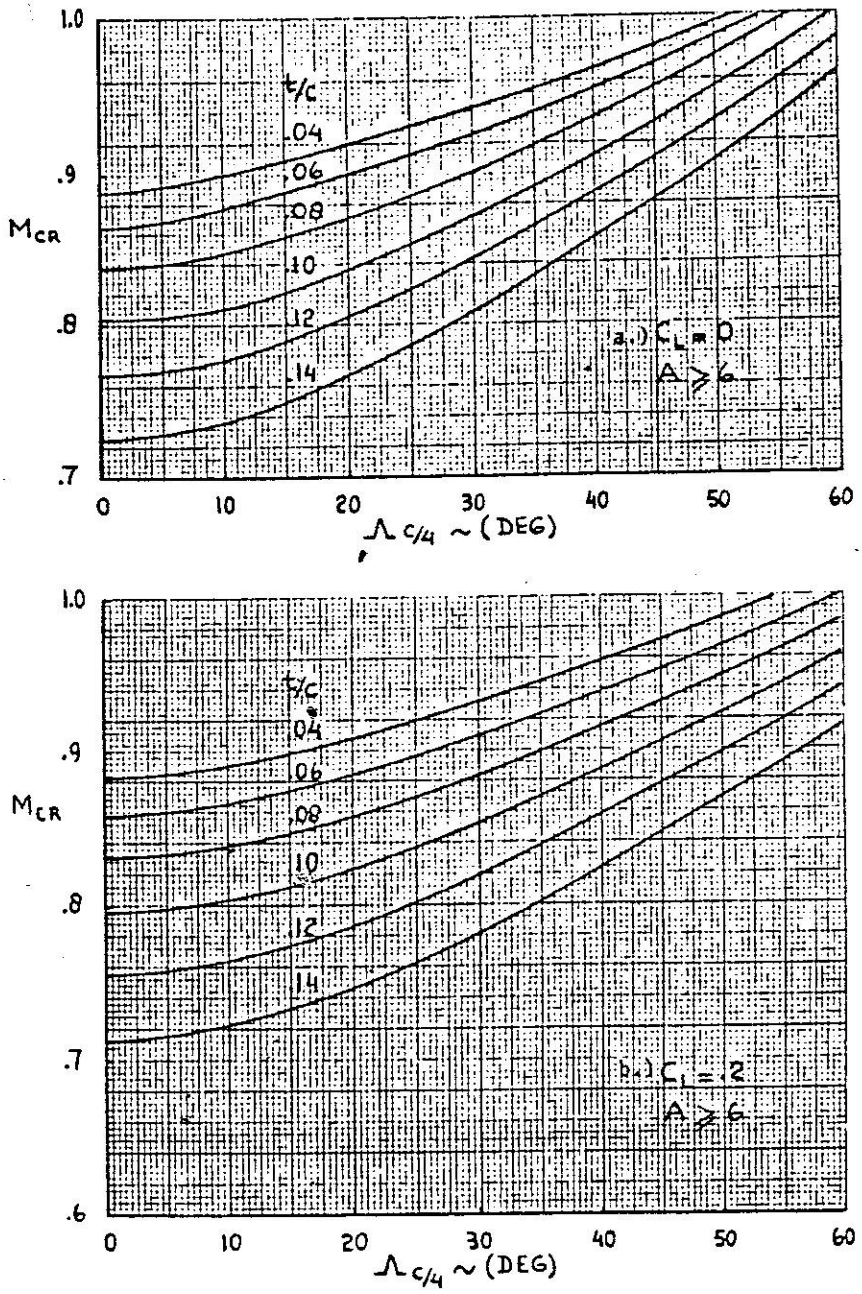

Figura 6.1a *Effetto del massimo spessore percentuale e dell'angolo di freccia sul numero critico di Mach*

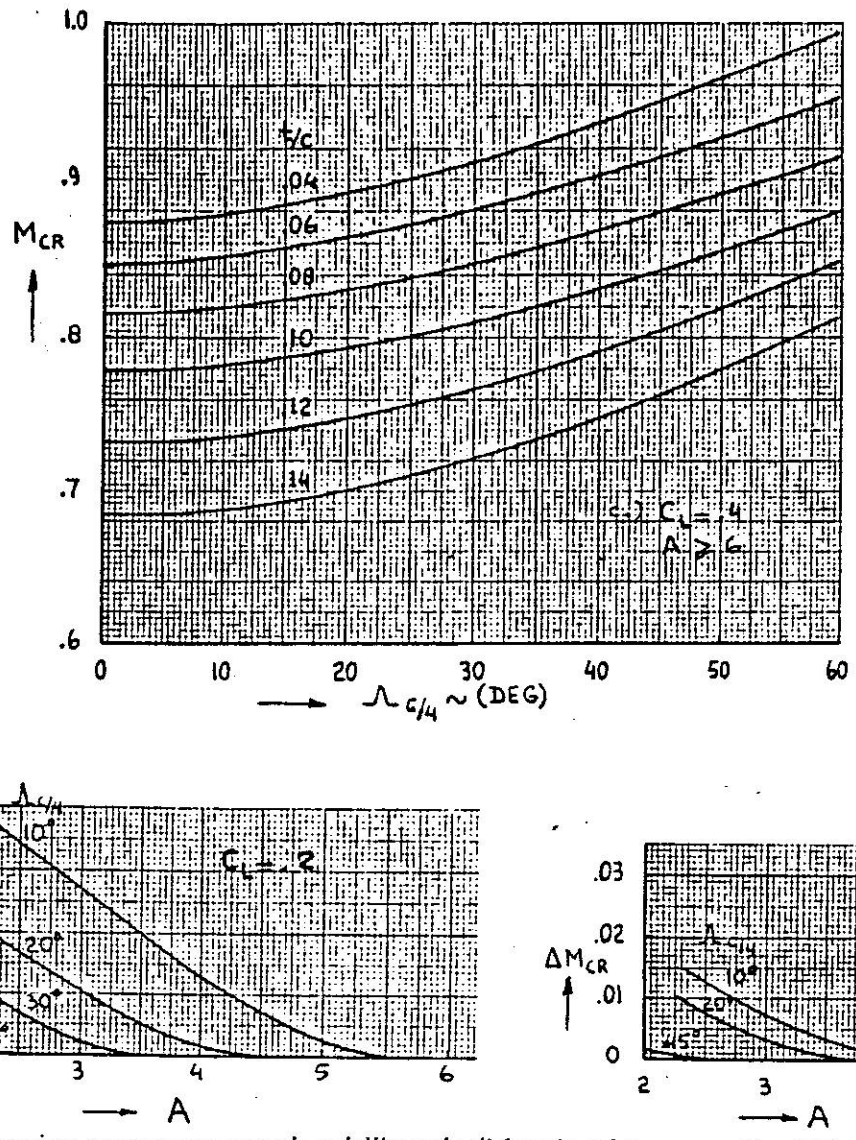

Figura 6.1b *Effetto del massimo spessore percentuale e dell'angolo di freccia sul numero critico di Mach*

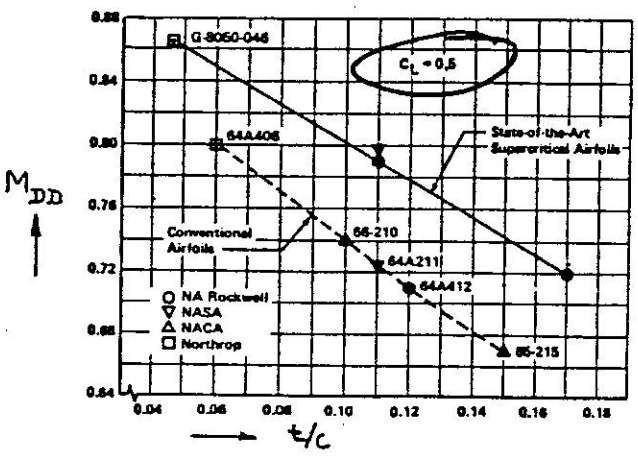

VERY ROUGHLY:

$M_{DD} = M_{CR} + 0.1$

Figura 6.2 *Effetto del massimo spessore percentuale sul numero di Mach di divergenza per alcuni profili NACA e supercritici*

Of greater practical interest is the so–called drag divergence Mach number, M_{dd} . This was also defined in Chapter 3 for an airfoil. Two definitions were given: the Boeing and Douglas definition respectively. These definitions are repeated next, as applied to the entire airplane.

a) Boeing Definition

M_{dd} is that free stream Mach number for which the drag due to compressibility first reaches 20 drag counts ($\Delta C_D = 0.0020$) above the incompressible level.

b) Douglas Definition

M_{dd} is that free stream Mach number for which the slope of the dragrise, $\delta C_D/\delta M$, first reaches the value 0.10.

These definitions are most easily applied when the drag rise behavior of airplanes is represented in a cross–plot of drag coefficient, at constant lift coefficient, versus Mach number. The reader is asked to apply these definitions to the dragrise behavior at different lift coefficients of the B–727–100 and the S–211 of Figure 5.3 and determine how closely they agree.

According to Chapter 4 (Figure 4.22), both critical Mach number and drag divergence Mach number depend strongly on the sweep angle. As it turns out, they also depend on the thickness ratio of lifting surfaces. These effects are illustrated in Figure 5.4 for conventional, non–super–critical airfoils.

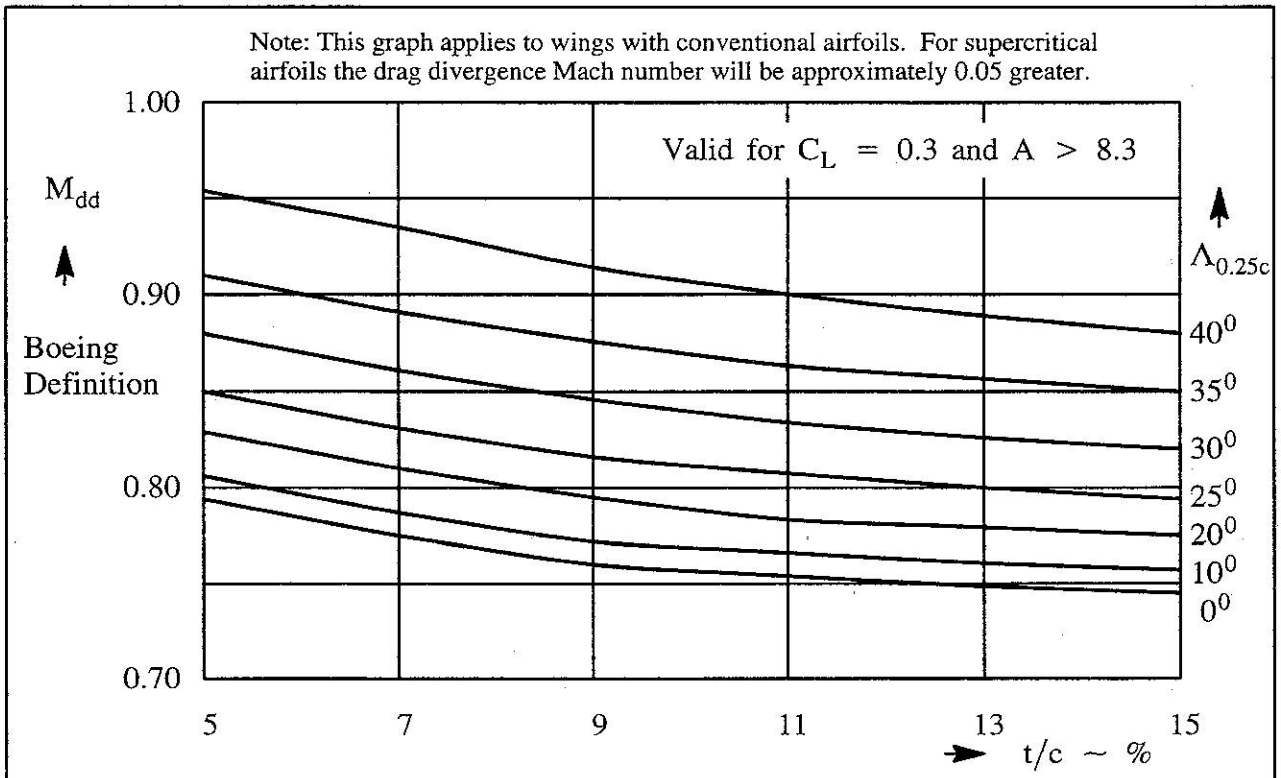

Figure 5.4 Effect of Wing Sweep and Thickness Ratio on Drag Divergence Mach Number

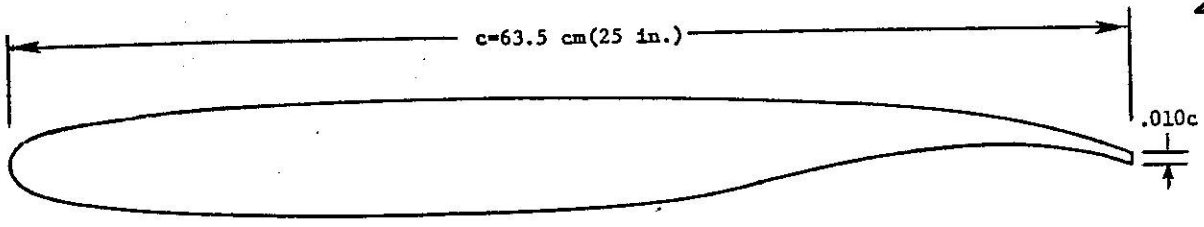

$(t/c)_{max}$ = 0.10

Basic Airfoil

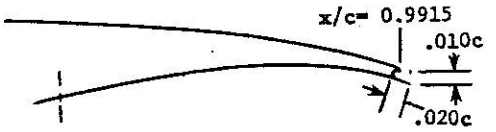

1.0- percent-thick trailing edge with cavity

Trailing-edge geometry for airfoil 9a

Figure 9.1.- Airfoil Geometry

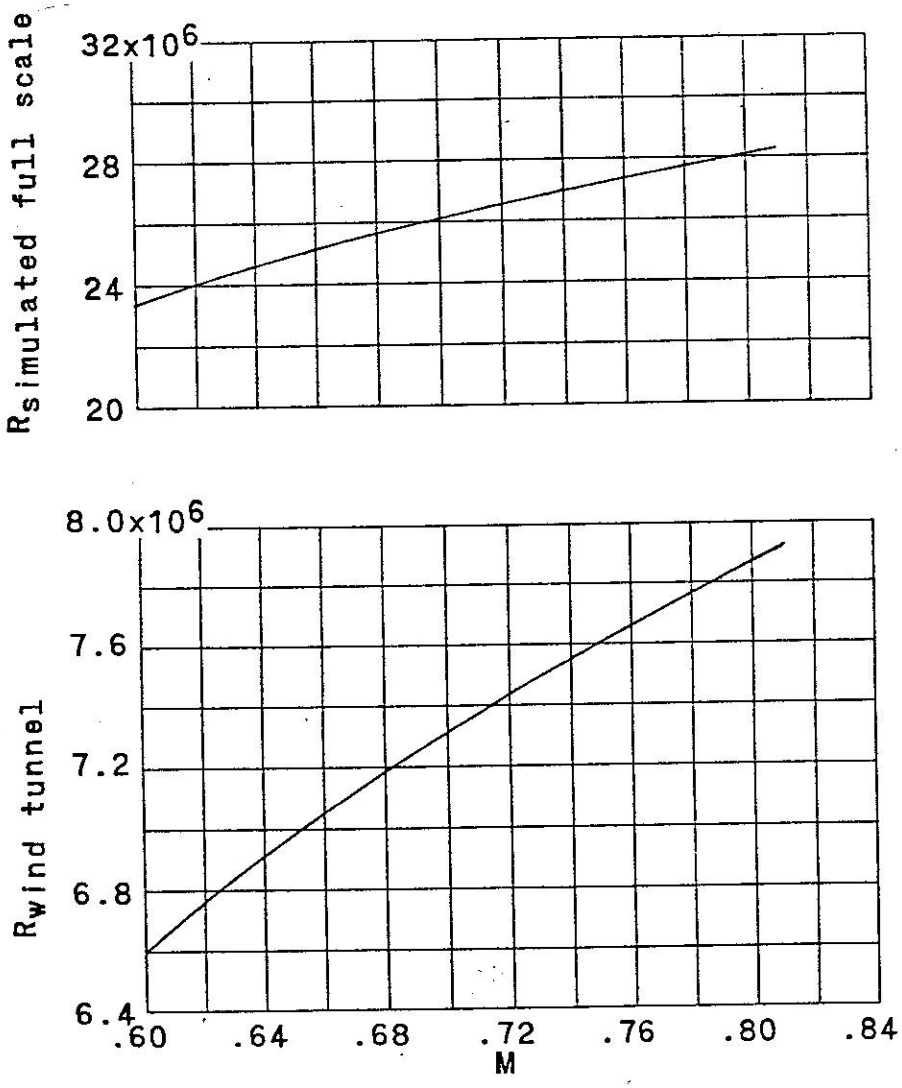

Figure 9.2.- Variation with Mach number of test wind-tunnel Reynolds number and simulated full-scale Reynolds number.

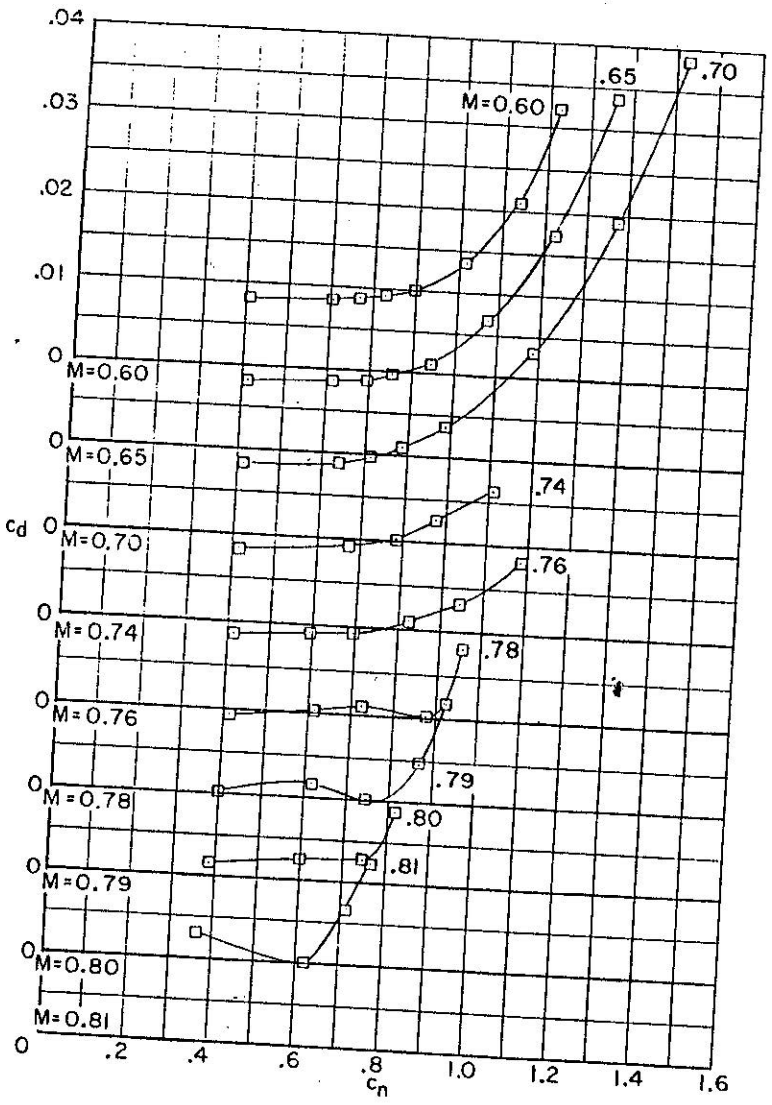

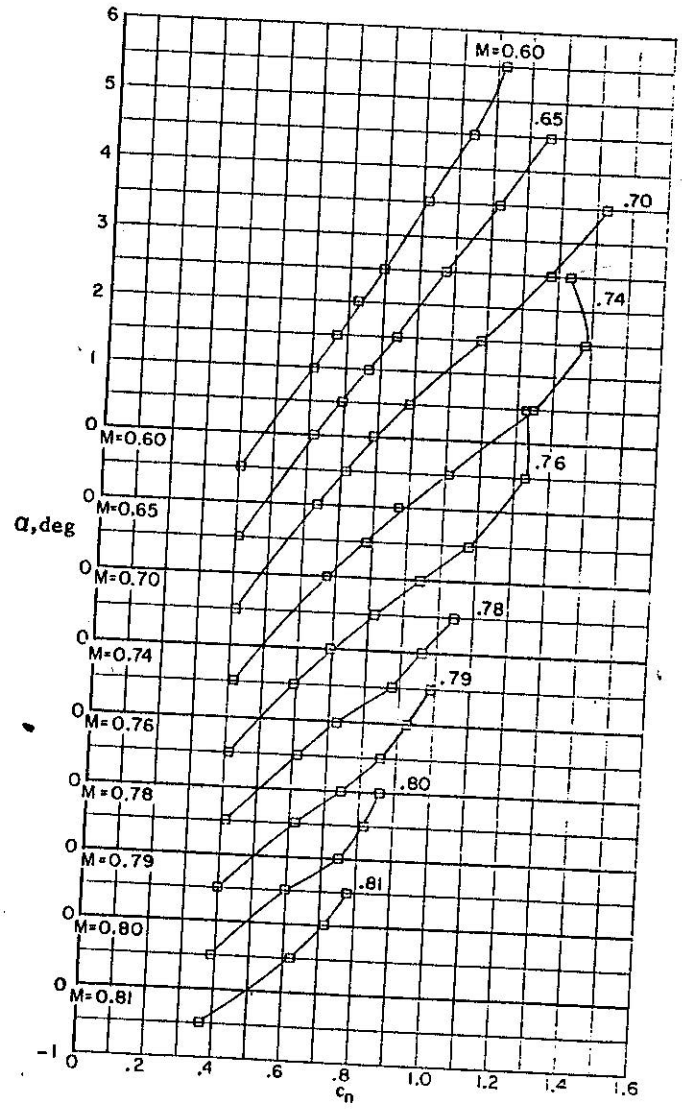

Figure 9.5.- Variation of section drag coefficient, angle of attack, and section pitching-moment coefficient at various Mach numbers.

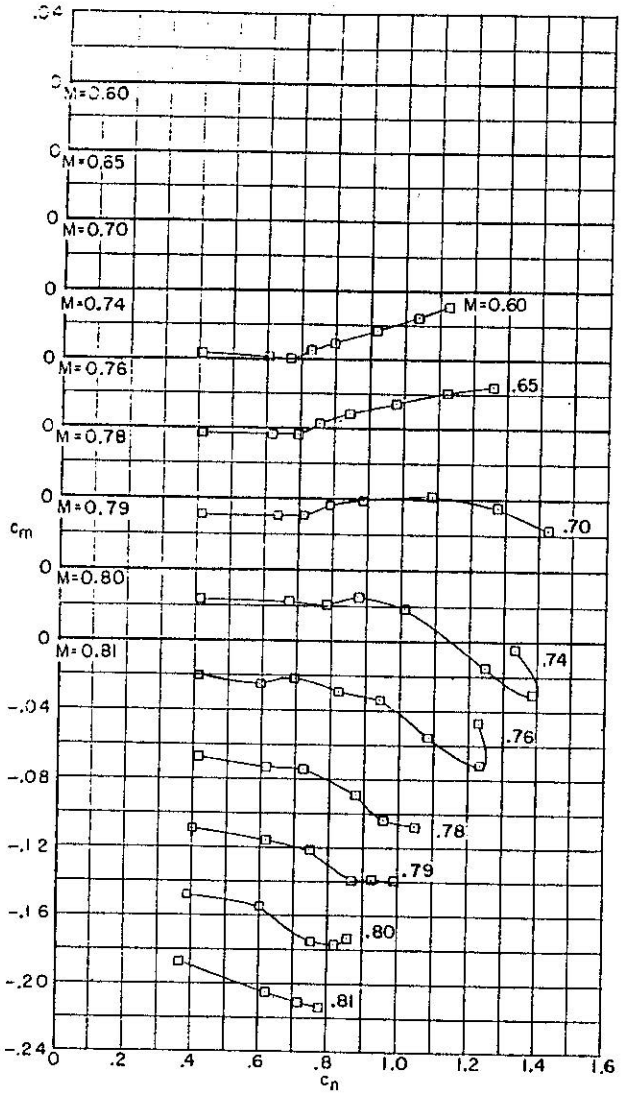

Figure 9.5.- Concluded.

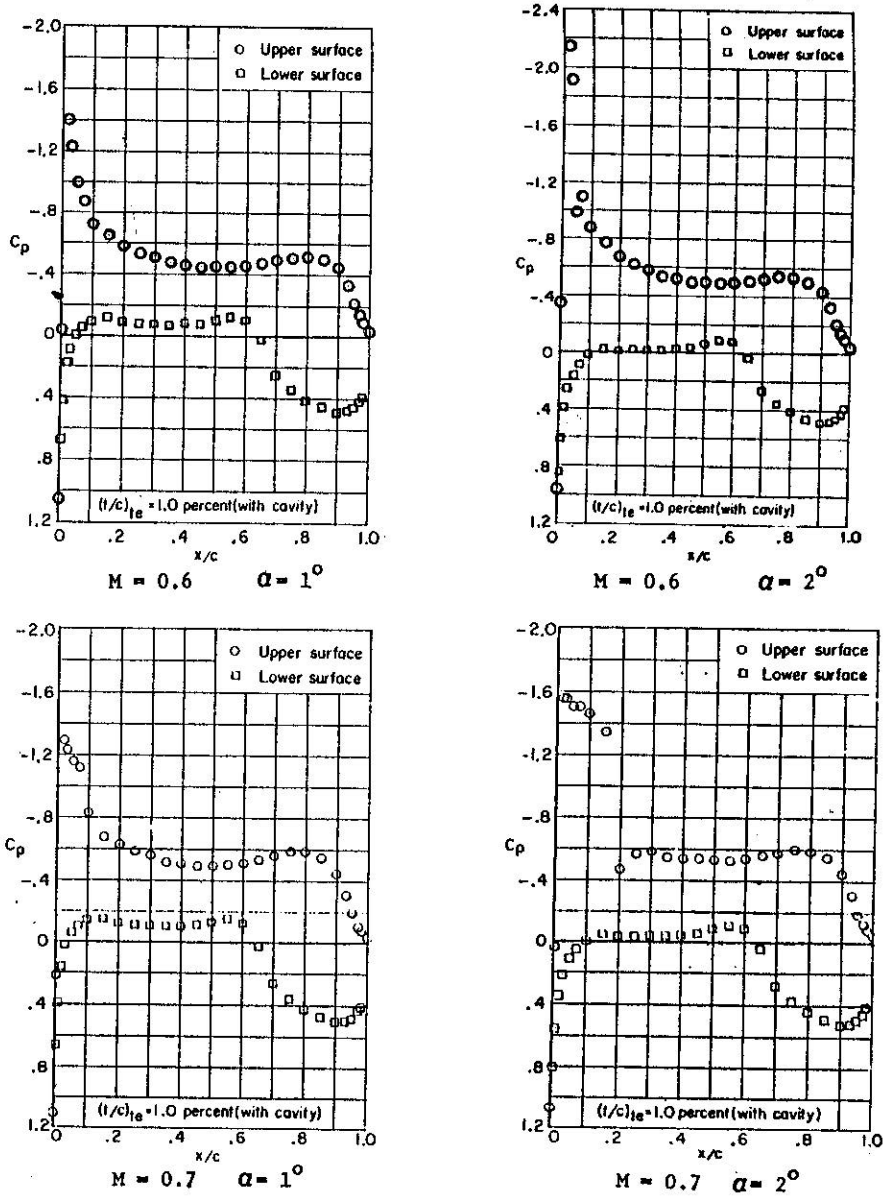

Figure 9.6.- Chordwise pressure distributions for various Mach numbers and angles of attack.

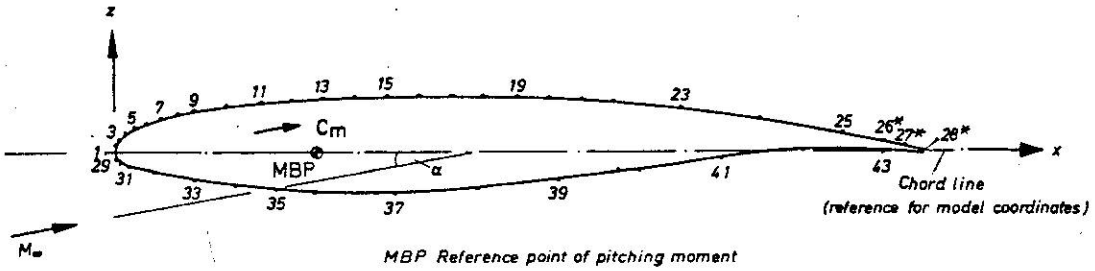

Geometric data: Chord c = 200 mm Maximum t/c = 11.8 % at x/c = 35 % Cross section $F_p \approx 3063 mm^2$
Trailing edge thickness $z_{TE}/c = 0.38\%$ Diameter of pressure orifices $d_B = 0.5$ mm

a. Contour and location of pressure orifices

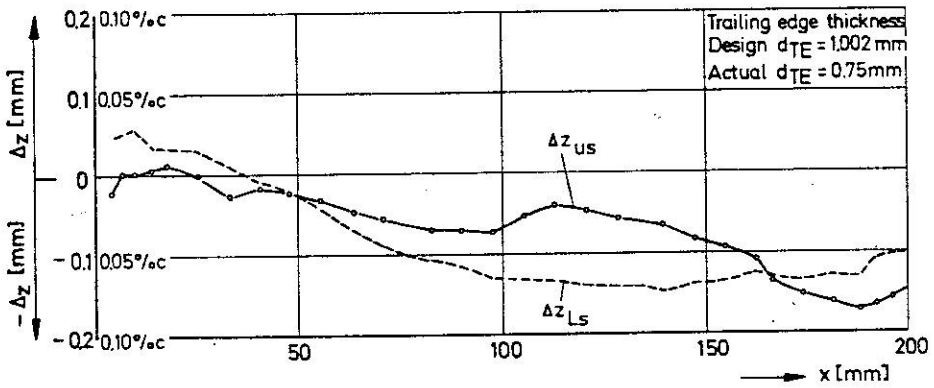

b. Measured error of manufactured airfoil (also see Table 3.1a)

Figure 3.1 Airfoil CAST 7 - Model SP 120 (c = 200 mm): Contour, location of pressure orifices and deviation from design coordinates (see Table 3.1b for deviation on ARA model)

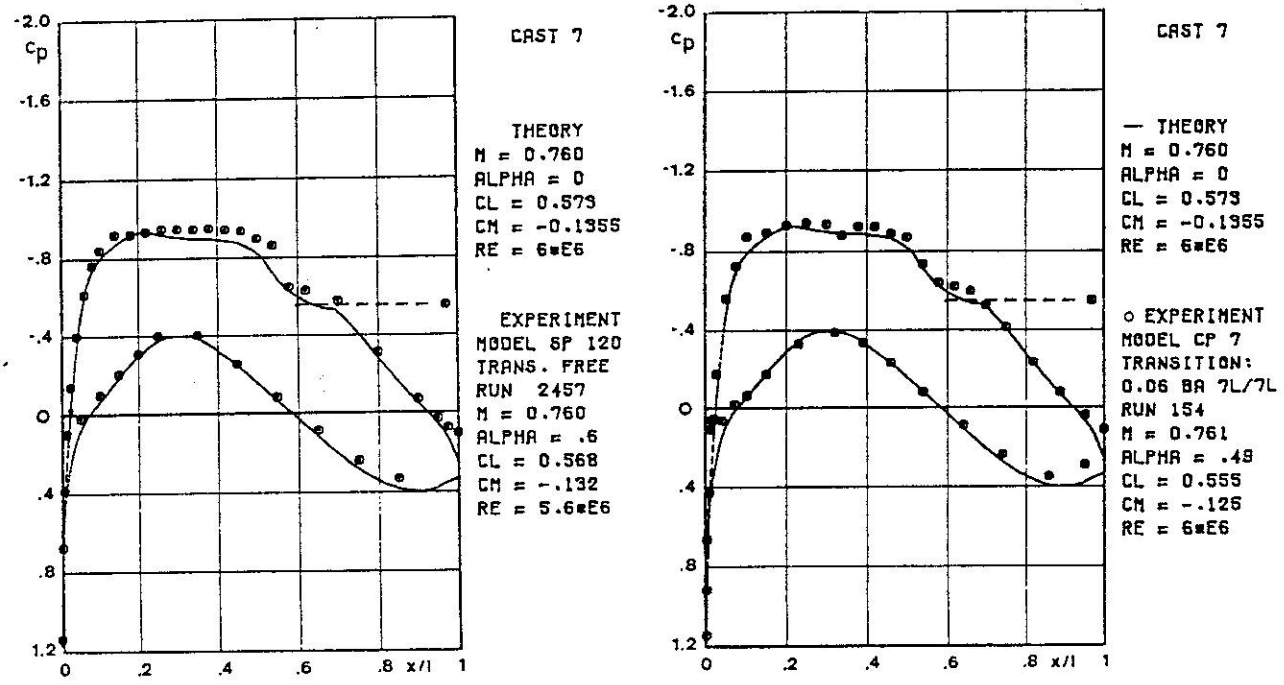

a. DFVLR - TWB tests b. ARA tests

Figure 3.2 Design pressure distribution. Comparison between theory and experiment.